sustainability

MDPI

Article

A Particle Swarm Optimization–Adaptive Weighted Delay Velocity-Based Fast-Converging Maximum Power Point Tracking Algorithm for Solar PV Generation System

Md Adil Azad [1], Mohd Tariq [2,*], Adil Sarwar [1,*], Injila Sajid [1], Shafiq Ahmad [3], Farhad Ilahi Bakhsh [4] and Abdelaty Edrees Sayed [3]

[1] Department of Electrical Engineering, ZHCET, Aligarh Muslim University, Aligarh 202002, India; mdadilazad2000@gmail.com (M.A.A.); injila.sajid123@gmail.com (I.S.)
[2] Department of Electrical and Computer Engineering, Florida International University, Miami, FL 33174, USA
[3] Industrial Engineering Department, College of Engineering, King Saud University, Riyadh 11421, Saudi Arabia; ashafiq@ksu.edu.sa (S.A.); aesayed@ksu.edu.sa (A.E.S.)
[4] Department of Electrical Engineering, National Institute of Technology, Srinagar 190006, India; farhad@nitsri.ac.in
* Correspondence: tmohd@fiu.edu (M.T.); adil.sarwar@zhcet.ac.in (A.S.)

Abstract: Photovoltaic (PV) arrays have a considerably lower output when exposed to partial shadowing (PS). Whilst adding bypass diodes to the output reduces PS's impact, this adjustment causes many output power peaks. Because of their tendency to converge to local maxima, traditional algorithms like perturb and observe and hill-climbing should not be used to track the optimal peak. The tracking of the optimal peak is achieved by employing a range of artificial intelligence methodologies, such as utilizing an artificial neural network and implementing control based on fuzzy logic principles. These algorithms perform satisfactorily under PS conditions but their training method necessitates a sizable quantity of data which result in placing an unnecessary demand on CPU memory. In order to achieve maximum power point tracking (MPPT) with fast convergence, minimal power fluctuations, and excellent stability, this paper introduces a novel optimization algorithm named PSO-AWDV (particle swarm optimization–adaptive weighted delay velocity). This algorithm employs a stochastic search approach, which involves the random exploration of the search space, to accomplish these goals. The efficacy of the proposed algorithm is demonstrated by conducting experiments on a series-connected configuration of four modules, under different levels of solar radiation. The algorithm successfully gets rid of the problems brought on by current traditional and AI-based methods. The PSO-AWDV algorithm stands out for its simplicity and reduced computational complexity when compared to traditional PSO and its variant PSO-VC, while excelling in locating the maximum power point (MPP) even in intricate shading scenarios, encompassing partial shading conditions and notable insolation fluctuations. Furthermore, its tracking efficiency surpasses that of both conventional PSO and PSO-VC. To further validate our results, we conducted a real-time hardware-in-the-loop (HIL) emulation, which confirmed the superiority of the PSO-AWDV algorithm over traditional and AI-based methods. Overall, the proposed algorithm offers a practical solution to the challenges of MPPT under PS conditions, with promising outcomes for real-world PV applications.

Keywords: PSO-adaptive weighted delay velocity (PSO-AWDV); maximum power point tracking (MPPT); photovoltaic (PV); DC–DC converter; hardware-in-the-loop (HIL)

check for updates

Citation: Azad, M.A.; Tariq, M.; Sarwar, A.; Sajid, I.; Ahmad, S.; Bakhsh, F.I.; Sayed, A.E. A Particle Swarm Optimization–Adaptive Weighted Delay Velocity-Based Fast-Converging Maximum Power Point Tracking Algorithm for Solar PV Generation System. *Sustainability* **2023**, *15*, 15335. https://doi.org/10.3390/su152115335

Academic Editors: Dinh Hoa Nguyen, Hung Dinh Nguyen, Javad Khazaei and Bowen Zhou

Received: 10 August 2023
Revised: 6 October 2023
Accepted: 23 October 2023
Published: 26 October 2023

Copyright: © 2023 by the authors. Licensee MDPI, Basel, Switzerland. This article is an open access article distributed under the terms and conditions of the Creative Commons Attribution (CC BY) license (https://creativecommons.org/licenses/by/4.0/).

1. Introduction

Global energy demand is rising due to the increase in the human population. In response to the growing population's needs, scientists and researchers have directed their focus towards renewable energy sources such as solar power, wind energy, geothermal energy, biomass, and more. Conventional sources of energy have a very negative impact

on the environment as well as on human health, and they are also limited in nature. Hence, renewable sources of energy are in practice nowadays. Among these renewable energy sources, solar is anticipated to be an important source of energy in most countries. Due to its long-term economic prospects, the abundance of input energy, durability, sustainability, pollution-free, and ease of maintenance, the photovoltaic (PV)-based power system is particularly becoming more popular as a renewable energy source [1].

When sunlight is incident on solar cells, they produce direct current (DC) power. In order to increase power generation, multiple solar cells are connected together to form a photovoltaic (PV) module. These modules can be further combined to create a solar array. However, the efficiency of PV modules is relatively limited due to the nonlinear characteristics of solar cells. Therefore, it is vital to optimize the power output of PV modules and maximize the amount of power they can generate.

In PV systems, homogeneous light intensity is frequently not possible due to atmospheric factors such as array tilt angle, bird droppings, sun direction, and shading due to buildings and clouds, which is known as partial shading (PS). This is a major drawback of the PV system. Additionally, PS might result in the creation of hotspots due to an excessive amount of heating at one point and may eventually harm the PV system. To mitigate the impact of heating and power loss, the bypass diode is linked in parallel with a photovoltaic (PV) system. Further, due to the use of a bypass diode under PS conditions, several peaks are created which decrease the output power and produce complex characteristics. Numerous optimization approaches have been proposed in various studies in the literature to ascertain the highest value from possible peaks.

2. Literature Survey

In the past decade, significant research has been dedicated to developing and implementing advanced algorithms in order to optimize power generation through maximum power point tracking (MPPT) in photovoltaic (PV) systems. The focus has been on devising effective techniques that enhance the efficiency of power generation. These studies have examined and compared various MPPT techniques based on factors such as efficiency, speed of convergence, simplicity, and cost.

Metaheuristic algorithms offer a robust and versatile approach to solving the MPPT problem, making them a popular choice of researchers and for practical applications in the field of solar energy. Researchers can select and customize specific metaheuristic algorithms based on the requirements of their MPPT systems and the specific challenges they aim to address. Metaheuristics work through an iterative process, starting with an initial solution and then iteratively improving it. These algorithms often incorporate randomness to escape local optima and efficiently explore a broader solution space. They rely on an objective function to measure solution quality and adapt their search strategies during optimization. Some of the latest metaheuristic algorithms such as the Mountain Gazelle Optimizer (MGO) [2], Giant Trevally Optimizer (GTO) [3], and Remora Optimization Algorithm (ROA) [4].

In Ref. [2], a mountain gazelle optimizer (MGO) was presented as a novel metaheuristic algorithm inspired by wild mountain gazelles' social behaviors and hierarchies. MGO leverages these natural traits through mathematical formulations to develop an innovative optimization algorithm. The study extensively evaluates MGO across fifty-two standard benchmark functions and seven distinct engineering problems, subjecting it to comparisons with nine other powerful meta-heuristic algorithms through statistical tests like Wilcoxon's rank-sum and Friedman's tests. In [3], the Giant Trevally optimizer (GTO) was presented as a novel metaheuristic algorithm inspired by the hunting strategies of the giant trevally in nature. The algorithm was developed based on mathematical models of the trevally's three main hunting steps, simulating their foraging movements, prey selection, and aerial attacks on seabirds. GTO's performance was rigorously assessed against state-of-the-art metaheuristics on a set of forty benchmark functions and five complex engineering problems.

Typically, MPPT techniques can be categorized into three groups: conventional approaches, artificial intelligence (AI) methods, and stochastic-/nature-based methods. While conventional hill-climbing algorithms are easy to implement, their efficiency is limited. In order to address this, a modified hill-climbing algorithm was proposed in the literature [5] that prevents deviation from the maximum power point (MPP). Additionally, Ref. [6] implemented hill-climbing algorithms that used fuzzy-logic controllers, and conducted a comparative study of non-fuzzy hill-climbing and modified hill-climbing. The perturb and observe (P&O) algorithm is a widely used MPPT technique known for its low cost and easy implementation. However, it suffers from inherent limitations that result in unavoidable power losses. Moreover, ref. [7] summarized other conventional MPPT algorithms, including incremental conductance (INC), parasitic capacitance (PC), and constant voltage (CV) methods. A modified P&O algorithm for photovoltaic (PV) systems has demonstrated higher maximum output power and efficiency compared to conventional methods [8]. However, a major drawback of conventional algorithms is that in the presence of multiple peaks in PV characteristics under partial shading conditions, these algorithms may detect one of the local peaks rather than the maximum global peak, as noted in [9]. The second category of MPPT algorithms employs fuzzy logic controllers (FLC), and optimization techniques, such as artificial neural networks (ANN) and artificial intelligence (AI) [10]. A comparison between FLC- and ANN-based MPPT techniques shows that the ANN-based algorithms have a faster response and reduce oscillation frequency about MPP [11]. However, these AI-based algorithms place a large computation burden on the system and require periodic training [12]. Conventional optimization techniques are often unable to track MPP and become stuck at local maxima under partial shading conditions (PSC), while AI-based algorithms can track MPP under PSC but need to be trained using historical data and requiring excessive memory. Thus, to achieve an accurate MPP locus and reduce oscillations about MPP, metaheuristic and evolutionary algorithms with fast convergence are used. Stochastic optimization methods, inspired by natural phenomena or animal behavior, form the basis of the third group of MPPT algorithms [13]. In Ref. [14], the utilization of genetic algorithm (GA) modeling was explored for determining the maximum power point (PMP) of a photovoltaic (PV) system. This involves generating chromosomal data that represent PV voltage (VPV), current (IPV), and power (PPV). The selection process is carried out using a ranking method based on the fitness value, which is indicated by PPV. Genetic algorithm (GA) is discussed for obtaining the maximum power point (MPP) by generating chromosomal data representing PV voltage (VPV), current (IPV), and power (PPV). Selection is completed based on the fitness value represented by PPV. Differential evolution (DE) is similar to GA and uses random initialization, mutation, crossover, and evaluation to guide the search in the search space [15]. In Ref. [16], the authors suggested that an improved MPPT algorithm can be achieved by combining evolutionary algorithms (EA) and AI-inspired techniques. To verify this suggestion, a DE- and ANN-based algorithm is implemented and compared with the P&O conventional algorithm.

In Ref. [17], the authors investigated the performance of three MPPT algorithms—P&O, PSO, and Firefly Algorithm (FA) in solar PV systems under PSC. The simulation findings reveal that P&O is unreliable for MPPT under PSC. It has a tendency to converge towards local maxima instead of the required GMPP. In contrast, PSO and FA are more intelligent and efficient, and can easily track the GMPP. According to the study, both PSO and the firefly algorithm (FA) exhibit comparable efficiency, exceeding the P&O algorithm's performance. Hence, they are considered superior choices for MPPT in solar PV systems operating in partial shading conditions (PSC). The observed oscillations in the steady state of PSO and FA can be attributed to the limited capability of the linear proportional–integral controller to handle the substantial nonlinearity of solar PV systems and the associated boost converter. In Ref. [18], the authors proposed a comparison of various MPPT techniques for solar PV systems and evaluated their performance in terms of accuracy, stability, speed, and cost. P&O and INC techniques are simple to implement but suffer from oscillations and power waste around MPP. The fuzzy logic controller (FLC) method is stable and

fast but more expensive to implement. In terms of adaptability and performance in diverse conditions, the adaptive neuro–fuzzy inference system (ANFIS) method outperforms both fuzzy logic control (FLC) and previous techniques. It demonstrates superior robustness and effectiveness. The hybrid approach combining neural network and P&O methods shows the fastest and most precise tracking of MPP, making it suitable for massive PV farms and fluctuating atmospheric conditions. However, its implementation requires proper training of the neural network and may be more expensive. The selection of the most suitable MPPT technique relies on factors such as specific application requirements, cost effectiveness, and the desired level of accuracy. In Ref. [15], the authors reviewed MPPT algorithms and proposed a new classification of four categories: measurement-based, calculation-based, intelligent scheme-based, and hybrid scheme-based methods. The studies on traditional and intelligent algorithms have been well-documented, and new methods and optimization have the potential for improvement. The use of metaheuristic methods and high-gain DC–DC converters should also be considered. A case study conducted on a photovoltaic (PV) system demonstrated that the fuzzy-PI algorithm combined with the single-ended primary inductor converter (SEPIC) outperformed alternative methods. The study concluded that there was still potential for enhancing the speed, accuracy, and flexibility of MPPT control systems across different operating conditions. Additionally, in Ref. [19], the authors proposed a hybrid nonlinear controller, combining the incremental conductance (INC) algorithm and integral backstepping technique, for efficient control and maximum energy harvesting in photovoltaic (PV) systems operating in dynamic conditions. The hybrid MPPT controller surpasses recently published MPPT methods, demonstrating a fourfold improvement in tracking the maximum power and achieving higher energy yield compared to the INC algorithm. The system is evaluated under consistent irradiance conditions, suggesting the need for future research to extend the application of the hybrid MPPT controller to PV systems operating under partial shading scenarios.

In order to integrate a PV-based MPPT with grid supply, it needs to combine particle swarm optimization (PSO) along with ANFIS, which is presented in [20]. The MPPT created using these methods has been found to be helpful in a number of real-world situations [20,21]. Because of their stochastic character, metaheuristic algorithms have the benefit of completing their search process by searching the search space. The algorithm then searches that space for the optimal solution. In [4], a Remora optimization algorithm (ROA) was demonstrated as a new method for maximum power point tracking (MPPT) in photovoltaic (PV) systems, specifically in partial shading conditions. The ROA is compared to other optimization algorithms in terms of power extraction, efficiency, and tracking rate. The results demonstrate that the ROA outperforms other methods in terms of efficiency and convergence accuracy, achieving a tracking efficiency of 99.97% and extracting higher power. The optimized ROA is a fast optimization technique for increasing PV system effectiveness in both normal and shaded situations. In Ref. [22], a dandelion optimizer (DO) algorithm was presented for maximum power point tracking (MPPT) in photovoltaic (PV) arrays under partial shading conditions. The DO algorithm outperforms other state-of-the-art algorithms in terms of power tracking efficiency, tracking duration, and maximum power tracking. The DO algorithm is a bioinspired stochastic optimization technique that models dandelion seed flight dynamics and offers superior productivity, speed, simplicity, and stability. In Ref. [23], the authors explored the use of particle swarm optimization (PSO) optimized with an adaptive network-based fuzzy inference system (ANFIS) to predict the ultimate bearing capacity of strip footings on sloping crests. The researchers compared the effectiveness of the PSO-ANFIS model with the ANFIS model in predicting the bearing capacity. They also conducted a parametric study on the most influential parameter of the PSO-ANFIS model. The results showed that the PSO-ANFIS model accurately predicted the bearing capacity, outperforming the ANFIS model. Meanwhile, Ref. [24] presented a voice-based drowsiness detection system using the Gray Wolf optimizer (GWO) and an artificial neural network (ANN). The proposed GWO-ANN method achieved higher accuracy in detecting driver drowsiness compared to other algorithms. The system

combines feature extraction techniques, dimension reduction, and machine learning for classification. The paper also discusses related works on emotion recognition and the use of swarm optimization techniques in pattern recognition. In Ref. [25], the authors focused on optimizing the performance of PV cells by developing a hybrid MPPT control strategy based on robust integral backstepping. It aims to continuously operate the PV system at its maximum power point, which depends on meteorological conditions. The strategy uses an ANFIS network to generate a reference peak power voltage and adjusts the power converter's duty ratio to achieve this set point, ensuring efficient and precise control without overshooting. MATLAB/Simulink R2019a simulations demonstrate its effectiveness, outperforming other MPPT strategies in various conditions. The authors of [26] introduced a novel hybrid MPPT control strategy for PV modules, combining sensor-less observer techniques with backstepping super-twisting sliding mode control (BSTSMC). This approach, aided by Gaussian process regression (GPR) for reference voltage generation and a differential flatness approach (DFA) with a generalized super-twisting algorithm (GSTA) for state retrieval, exhibits superior MPPT performance. Simulations in MATLAB/Simulink under various conditions show that it offers a rapid dynamic response, finite-time convergence, minimal chattering, high tracking accuracy, and robustness against uncertainties, load disturbances, and certain system faults compared to benchmarked and conventional MPPT strategies. The authors of [27] concluded that a nonlinear robust backstepping-based MPPT control technique could significantly outperform linear MPPT methods, such as conventional PID and P&O, especially in scenarios involving varying atmospheric conditions and system faults. This highlights the importance of nonlinear MPPT controllers for improving the efficiency and performance of standalone PV arrays connected to dynamic loads.

The effectiveness of these algorithms can vary based on factors such as the settling time to reach the maximum power point (MPP), the occurrence of power fluctuations during MPP tracking, efficiency compared to the true MPP, the impact on processor memory load, and other related aspects. To further improve existing MPPT methods and enhance their affordability, there is a need to develop algorithms that offer higher performance while maintaining simple structures, and minimizing the number of variables stored in processor memory. An ideal system is one in which the least expensive components are employed without degrading the system's performance. Unlike complicated algorithms that may cause the less costly processors to fail and necessitate the employment of an expensive solution because there are too many updating equations. On the other hand, a straightforward algorithm structure will exert minimal pressure on the memory of the processor, making it the most suitable option for less costly processors. As a result, the best algorithm is one that improves system performance with respect to the previously mentioned factors, such as tracking time, efficiency, etc., while also placing the least amount of strain on the CPU. Thus, there is a need for ongoing study in this field using straightforward structured algorithms that may satisfy all of the criteria for the perfect algorithm, which makes the system more affordable and dependable. Several researchers have utilized particle swarm optimization (PSO) with various modifications for maximum power point tracking (MPPT) due to its simple structure. Table 1 provides an overview of previous research endeavors within the realm of maximum power point tracking (MPPT) techniques [28–41].

Table 1. Shows previous research in the area of MPPT techniques.

Reference	Strategies Involved	DC–DC Converter	Findings/Remarks
[8]	Scales that are conventional, two steps in size, and changeable steps P&O	Boost Converter	• The variable-step and two-step techniques can be used to manage an imbalance between dynamic performance and steady-state performance. • Enhanced stability in the event of an external atmospheric change. • The MPP is tracked by modified algorithms in 50% less time than with regular P&O.
[28]	Combining voltage-directed current regulation with momentum-based P&O	Boost Converter	• Utilizing current control results in a quick reaction to irradiation fluctuations that occur quickly. • Using a storage variable makes switching to classic P&O simple. • Oscillations were reduced by 30%, and the following speed was doubled.
[29]	FOCV strategies using semi-pilot cells (SPC) and semi-pilot panels (SPP)	Buck–Boost converter	• SPC replacement of the pilot cell during open-circuit voltage monitoring helps to reduce power loss. • The algorithms SPC FOCV MPPT and SPP FOCV may properly evaluate the V_{MPP}. As a result, the PV system's total efficiency is increased. • It is not intended for SPP-FOCV to be used during PSCs.
[30]	Improved FOCV technique	Buck Converter	• Regular open-circuit voltage checks increase the effectiveness of the algorithm by temporarily reducing the amount of energy that can be drawn from the PV panel and assisting in a crucial changeover process to the converter. • When a change in V_{oc} results from a change in temperature, it is effective. • Voltage and load are sensed by a single sensor.
[31]	PSO + FLC MPPT	Boost converter	• The PSO strategy determines the controllers' gain in the PSO-Fuzzy approach. • In comparison to conventional approaches, the proposed hybrid algorithm runs at a fast-tracking speed and exhibits less oscillation.
[32]	New pheromone update-based ant colony optimization (ACO-NPU)	Buck–Boost converter	• In the midst of the search phase, the ACO NPU method renews the pheromone, moving the ants towards the GMPP. • For search advancement, the suggested technique uses a sporadic dispersal look. • The suggested approach shows improvements over the conventional ACO in terms of tracking speed and accuracy.
[33]	SSO MPPT strategy	Buck–Boost converter	• The proposed SSO method is 20–30% faster than the conventional approaches like PSO, CS, ABC, etc. • The suggested method can conserve electricity in a transitory condition due to its quick settling periods and quick tracking speeds. • Additionally, it avoids problems like overshoot and ripples.
[34]	FSSO MPPT strategy	Quasi-Z-source Converter	• The FSSO technique accelerates convergence when the predator is not realized. • The suggested algorithm's tracking effectiveness is often the highest. • The provided approach is system agnostic since it may be used with various infrastructures.
[35]	OSA+ INC MPPT strategy	Boost converter	• The suggested hybrid system increases convergence speed and, with a little adjustment, properly monitors the MPP under typical temperature settings. • The method is simple to implement and avoids oscillations at the MPP.

Table 1. *Cont.*

Reference	Strategies Involved	DC–DC Converter	Findings/Remarks
[36]	Modified FA MPPT method	Boost Converter	• By progressively lowering the algorithm constants used in each iteration, the modified FA method accelerates convergence. • During the PSC condition, the suggested method's average efficiency is higher than 99.98%.
[37]	Generalized Bell (GBell) membership function + FLC MPPT approach	High gain voltage DC–DC converter	• The GBell function outperforms additional fuzzy membership operations in terms of tracking speed, oscillations, and converter output optimization. • For solar photovoltaic systems, the GBell membership function's design gives exceptional performance.
[38]	Fuzzy-based Strategy	Boost converter	• The proposed fuzzy control method operates over the PV array's whole width in the stable zone. As a result, it gets rid of the variations around the MPP. • For more procedures involving ambiguous membership, a microcontroller for converters might be used to carry it out effectively.
[39]	Feed-forward weight update combined with the INC training technique	Boost converter	• A powerful power converter and a soft-computer MPPT controller can boost a PV system's efficiency. • A strong steady-state responsiveness and fewer transients are shown by the updated approach.
[40]	GA + ACO	Boost converter	• In order to prevent tapping in local maxima, ACO scans the sub-space. • GA is used to find a practical solution and prevent premature convergence. • The convergence time of the hybrid GA-ACO methodology is half that of the GA and ACO techniques.
[41]	Strategies using Whale Optimization (WO) and DE MPPT	Boost Converter	• While the DE approach lowers the meta-heuristic character and random constant effects, the WO technique exhibits a significant searching capacity in a broad search zone, leading to a fast convergence speed. • The hybrid technique is fast in all environmental conditions, system-independent, dependable, and not reliant on starting conditions.

In this paper, the PSO–adaptive weighted delay velocity (PSO-ADWV) algorithm has been proposed for solar PV-based MPPT. In order to evaluate the effectiveness of the PSO-AWDV algorithm, a comparative analysis is conducted with traditional PSO and PSO-VC (PSO variable-coefficient) algorithms. With respect to fewer fluctuations, tracking time, and resilience, the findings showed that PSO-AWDV performs better than the traditional PSO and PSO-VC algorithms. Further, due to its straightforward structure, it puts a low strain on processor memory, particularly when a cheap controller is used. The performance of the basic traditional PSO for MPPT needed to be improved. From the above literature review, it could be seen that while certain algorithms are fast, they converge prematurely while others show oscillation at MPP. To overcome the above problem, PSO-AWDV is proposed.

The main highlights of the PSO-AWDV algorithm are:

1. The PSO-AWDV algorithm has a simple formulation and has less computational complexity than conventional PSO and its variant PSO-VC.
2. It could locate the MPP for complex shading patterns including partial shading conditions and significant insolation fluctuations.
3. The efficiency of tracking is also very high and better than conventional PSO and PSO-VC.

This research article is structured in the following manner. Section 3 of the article presents the formulation and modeling of the photovoltaic (PV) framework. By examining I-V and P-V curves, Section 4 looks at how changes in solar irradiance affect the output

performance of the PV system. Section 5 of the article explains the partially shaded condition, while an overview of the photovoltaic (PV) system model framework and maximum power point tracker utilized in this investigation is given in Section 6. The implementation of the proposed PSO-AWDV-based maximum power point tracking (MPPT) algorithm and other metaheuristic algorithms employed in this work are described in detail in Section 7. In Section 8, the MATLAB/Simulink findings are assessed and contrasted. The results of the proposed PSO-AWDV algorithm for MPPT's real-time hardware-in-the-loop (HIL) implementation are shown in Section 9, along with a comparison to PSO and PSO-VC algorithms. Section 10 provides the suggested algorithm's potential future applications and Section 11 concludes the article.

3. Modelling of Photovoltaic (PV) System

Figure 1 illustrates a single-diode model. It is comprised of a single current source that is anti-parallel to a single diode, a series, and a shunt resistance that are connected to account for ohmic losses and for leakage resistance to the ground, respectively [25,42]. A two-diode model includes a number of factors that make a problem more difficult, despite the fact that it is more precise and can produce better outcomes. In contrast, the single-diode model simplifies PV cell modeling and yields reasonable approximations. Therefore, for PV modeling, using a single-diode model is preferred. A photovoltaic (PV) module is typically formed by combining multiple cells connected in series and/or parallel configurations. There are four modules linked in series in the current model. The temperature and the amount of solar irradiation have a significant impact on the PV model's features [43]. The series and parallel resistances also have an impact on the single-diode model features. The following mathematical Formula (1) is used to represent the PV cell output current:

$$I = I_P - I_{SAT}\left[exp\left(\frac{q(V_o + I \cdot R_{SE})}{a \cdot K \cdot T}\right) - 1\right] - \frac{V_O + I \cdot R_{SE}}{R_{SH}} \quad (1)$$

where I is the photovoltaic current; I_{SAT} signifies the diode saturation current; I_P photo denotes the diode current; I_{SH} is the current following through the parallel resistor; q stands for the electronic charge; V_O is the output voltage of the photovoltaic model; R_{SE} is series resistance; R_{SH} is the parallel resistance; ideality factor is denoted by n; Boltzmann's constant is K; the temperature of the cell in degree Celsius is denoted by T.

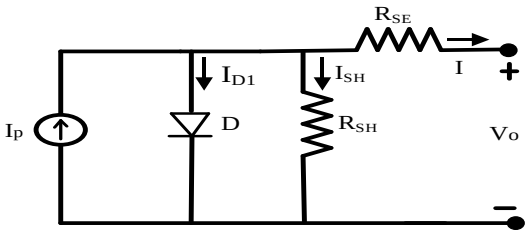


Figure 1. Equivalent circuit of a solar cell.

4. Solar Cell Characteristics

Short-circuit current (I_{sc}) is the current that flows through a solar cell when it is connected in a short-circuit configuration. Conversely, open-circuit voltage (V_{oc}) corresponds to the highest voltage achievable from a solar cell in a situation where no current is passing through it. It is crucial to understand that neither the short circuit nor the open circuit states actively contribute to the production of power. Nonetheless, there exists a particular pairing of current and voltage that optimizes the generation of maximum power (P_{max}). Figures 2 and 3 illustrate the behavior of a PV cell under constant temperature conditions at various levels of solar irradiance. Figure 2 presents the current-voltage characteristics, while Figure 3 showcases the power-voltage characteristics of the PV cell. The findings derived from these figures suggest that an increase in solar irradiance has a slight impact on the open-circuit voltage of the PV cell, while the short-circuit current experiences a

significant rise. As a result, the power output of the PV cell is directly affected by the level of insolation at a constant temperature.

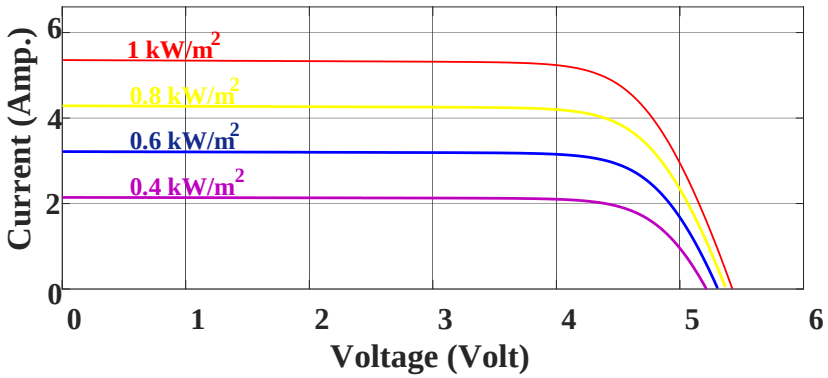


Figure 2. The impact of changing insolation on the solar cell's I-V properties.

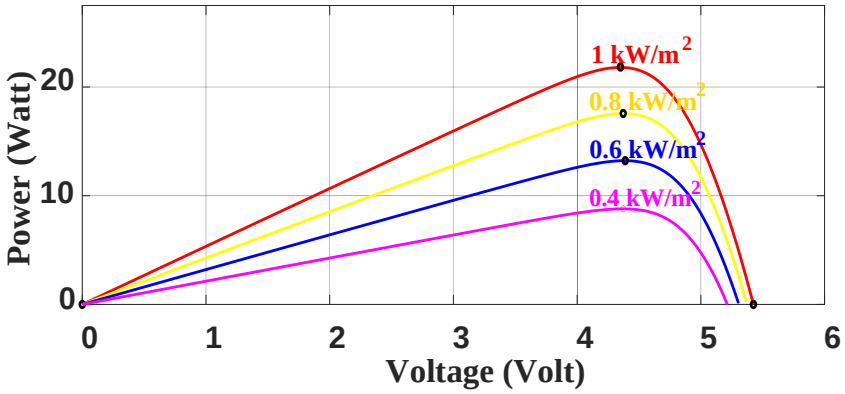


Figure 3. The effects of different insolation levels on the P-V characteristics of the solar cell.

5. PV Array under Partially Shaded Condition

A photovoltaic (PV) array refers to the interconnected arrangement of numerous PV modules, which are connected in series or parallel. This configuration is designed to enhance the power capacity of the PV array by increasing the voltage level through a series connection and improving the current level through a parallel connection. However, the illumination received by the series-connected PV modules is not uniform due to various factors such as neighboring structures, shadows from trees, movement of clouds, and so on. This leads to partial shading conditions (PSC) where the insolation on the panels becomes uneven. To solve these problems, bypass diodes and blocking diodes are used. Bypass diodes (D_{Byp}) in a solar PV system are used to mitigate the negative effects of shading and prevent damage due to reverse bias conditions. They create alternate paths for current when a solar cell is shaded, ensuring that other cells continue generating power and preventing excessive power loss. Blocking diodes (D_{Block}), on the other hand, are employed to prevent reverse current flow from the battery or load back into the solar panel, ensuring efficient energy transfer and protecting the system's components, particularly in off-grid systems with energy storage. Both types of diodes contribute to the overall efficiency and reliability of the solar PV system [44]. In this research, a PV system with four modules connected in series is examined. The graph in Figure 4 illustrates the power-voltage (P-V) characteristics of these four modules under non-uniform insolation. Due to the non-uniform insolation, there are four peaks observed, with one peak representing the global maximum and the other three being local maxima. The partial shading significantly affects the output of the entire series-connected PV module string [44,45]. The operational voltage of a shaded panel decreases, sometimes turning negative, resulting in energy dissipation due to the reverse-biased conditions.

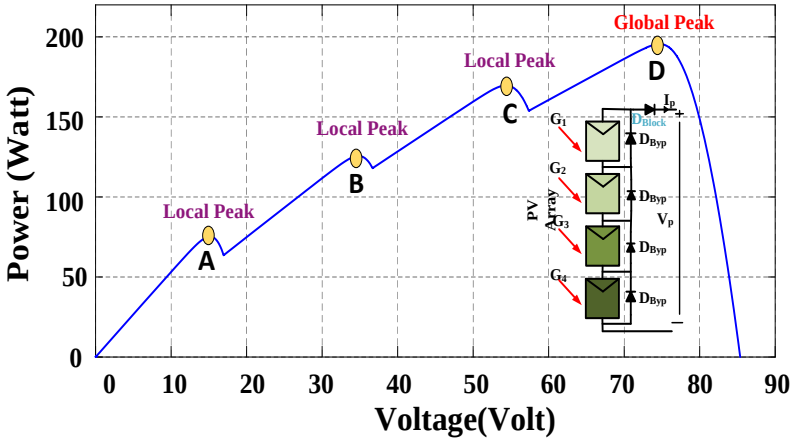


Figure 4. P-V characteristics for non-uniform insolation.

Conventional MPPT methods face a challenge in distinguishing between local maxima and global maxima, as both points exhibit zero slope. To address this issue, researchers have turned to metaheuristic-based optimization techniques, which are capable of exploring and exploiting the maximum point across the entire search space of solution vectors. Population-based metaheuristic techniques, such as particle swarm optimization (PSO), have emerged as a viable solution to this problem. The following section introduces improved variations of PSO, specifically designed to tackle the power tracking issue in solar PV arrays.

6. Maximum Power Point (MPP) Tracker

The MPP tracking system, illustrated in Figure 5, encompasses a closed-loop controller integrated with the help of sensors, a microcontroller, a driving circuit, and a DC-to-DC boost converter. The microprocessor measures the voltage and current of the PV array, computes the duty ratio value (DR_v), and sends the converter's tuning signal via the gate driver circuit. The MPPT algorithm is used by the controller to determine the best D_P values for ($P_{Max\ P}$) extraction from the PV array. The MPPT problem is formulated using Equation (2), which defines the objective function (z) for the optimization process.

$$f(DR_V) = P_{Max\ P} \tag{2}$$

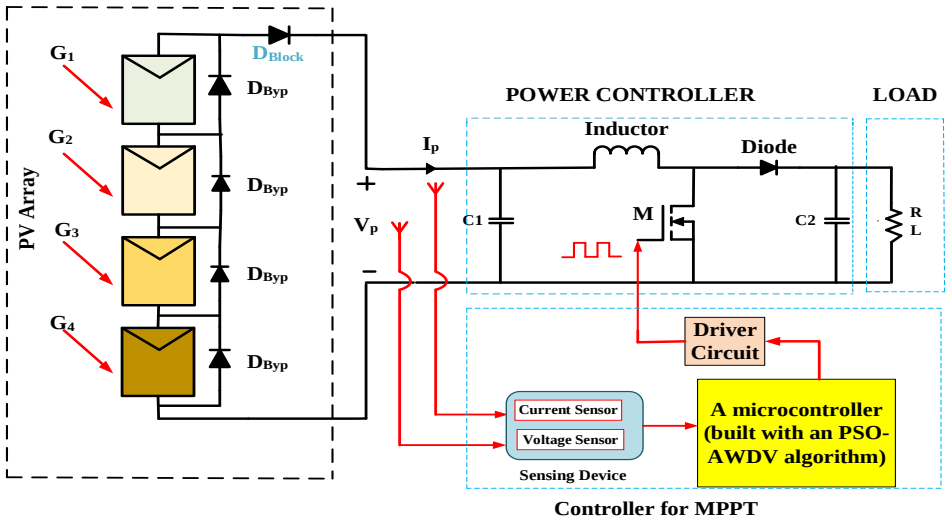


Figure 5. A photovoltaic (PV) system that uses a maximum power point (MPP) tracker built on a DC–DC boost converter.

The PSO-AWDV algorithm is employed in this study to identify the GMPP, which corresponds to the optimal value of (DR_V) leading to maximum power output ($P_{Max\ P}$).

7. MPPT Based on Metaheuristic Optimization Algorithms

In PV-generating systems, MPPT has been implemented using metaheuristic algorithms to successfully capture the GMPP and overcome the limitations of conventional approaches. These algorithms possess the capacity to thoroughly inspect the search space and identify the optimal global solution by leveraging their inherent exploitation capabilities, thus outperforming local optimization approaches. Consequently, the choice of optimization algorithm significantly impacts the effectiveness of the MPPT controller. It is crucial to consider a number of characteristics while creating an MPPT controller in order to make it both cost effective and power efficient. These parameters are:

- **Minimal failure rate**: There should be little chance of early convergence or failure for the MPPT algorithm. It is determined by dividing the total number of attempts by the number of efforts that converge to one of the MPPs.
- **Rapid convergence**: An economic MPP tracker should use fewer computing rounds since the MPPT method should soon settle at the MPP.
- **Consistent fluctuations**: The MPPT algorithm should possess dependable abilities for both exploring and exploiting the search space, avoiding unnecessary traversal of irrelevant regions. As a result, power fluctuations and related losses are decreased.
- **Resilience**: Even in the presence of significant oscillations under PS circumstances and abrupt dynamic changes in PV insolation, the GMPP should be recognizable by the MPPT algorithm.

In order to guarantee an MPPT controller's efficient functioning, it is important to investigate and employ advanced algorithms that can improve essential parameters such as convergence speed, minimize power fluctuations, and enhance computational efficiency.

Through the use of metaheuristic algorithms, the MPPT technique may be described. In this method, the MPPT issue may be resolved by adjusting the duty ratio of the DC-to-DC boost converter. The metaheuristic algorithm built into the microcontroller is first given starting power and duty ratios. After initializing the boost converter switch with the initial duty ratio values, the MPPT algorithm activates the switch through the gate driver circuit. The microcontroller analyzes the voltage (V_p) and current (I_p) measurements obtained from the sensors. During each iteration, the algorithm compares the newly calculated power with the previous power and records the duty ratio (DR_v) corresponding to the highest power. By iteratively evaluating different duty ratios and comparing their associated powers, the algorithm identifies the optimal duty ratio that maximizes power extraction for a specific combination of insolation.

7.1. Conventional PSO and Its Implementation

Kennedy and Eberhart first introduced the swarm-based stochastic algorithm known as PSO, which takes advantage of ideas from animals' social behavior like flocking of birds and schooling of fish [46,47]. Each potential solution in PSO is viewed as a particle traveling through the problem's space at a specific speed, much like the flocking of birds. Each of the particles then mixes a portion of its best location and present location with other swarm agents, along with some random disturbances, to decide its next course through space. The next iteration starts after every particle has been moved. PSO has shown itself to be highly effective in a broad range, with the ability to hybridize and specialize as well as exhibit certain endearing emergent behaviors. Each particle in the swarm moves toward its previous global best position (G_{Best}) and personal best (P_{Best}) position in order to reach the optimal outcome. Considering a minimization issue:

$$P^q_{Best\ t} = y_t | \text{fn}\ (y_t) = \text{minimum}\left(\left\{fn\left(y^k_t\right)\right\}\right) \quad (3)$$

here t ∈ {1, 2, . . ., N}, & k = {1, 2, 3, . . ., q}

$$G^{q}_{Best\ t} = y^{q} | \text{fn}\ (y^{q}\ ) = \text{minimum}\ \left(\left\{ fn\left(y^{k}_{t} \right) \right\} \right) \tag{4}$$

here t ∈ (1, 2, . . ., N) & k = {1, 2, 3, . . ., q}

where t is used for the particle index, the current iteration number is denoted by q; fn stands for the objective function to be optimized; y stands for the position vector; N is the actual number of particles in the swarm. The positions y and velocity v of each particle t are updated according to the following Equations (4) and (5) at each iteration $q + 1$:

$$v^{q+1}_{t} = \text{w}v^{q}_{t} + c_1 s_1 \left(P^{q}_{Best} - y^{q}_{t} \right) + c_2 s_2 \left(G^{q}_{Best} - y^{q}_{t} \right) \tag{5}$$

$$y^{q+1}_{t} = y^{q}_{t} + v^{q+1}_{t}, \tag{6}$$

where w is the inertia weight used to balance local exploitation and global exploration; v is the velocity vector; s_1 and s_2 are positive constants known as acceleration coefficients; the acceleration factors, which are also known as the cognitive and social parameters, are denoted by the letters c_1 and c_2, respectively.

7.2. PSO-Variable Coefficient (PSO-VC)

In this study, data from research that used the PSO in MPPT control units were tentatively analyzed and generalized as the analytical object, hence, modified PSO versions were used which demonstrated a high PV panel MPP tracking efficiency [45]. The variable coefficient PSO intended by the authors of [46] is one of these modifications:

$$w^{q} = w_{Max} - \frac{q}{q_{Max}} \times (w_{Max} - w_{Min}) \tag{7}$$

$$c^{q}_{1} = c_{1\ Max} - \frac{q}{q_{Max}} \times (c_{1\ Max} - c_{1\ Min}) \tag{8}$$

$$c^{q}_{2} = c_{2\ Min} + \frac{q}{q_{Max}} \times (c_{2\ Max} - c_{2\ Min}) \tag{9}$$

where w_{Max} and w_{Min} are upper and lower bounds of w, maximum iterations allowed are denoted by q_{Max}. The $c_{1\ Min}$, $c_{1\ Max}$, and $c_{2\ Min}$, $c_{2\ Max}$ are the lower and upper bounds of c_1 and c_2, respectively.

7.3. PSO–Adaptive Weighted Delay Velocity (PSO-AWDV)

Particle swarm optimization (PSO) achieves favorable outcomes through the interaction among particles. However, in search spaces with numerous dimensions, PSO tends to converge towards the global optimal solution at a sluggish pace. Additionally, it produces inferior results when confronted with intricate and sizable datasets. When dealing with problems that possess a large number of dimensions, PSO often fails to discover the global optimum. This can be attributed to the fluctuation in particle velocities, which restricts subsequent attempts within a subset of the overall search area, and the presence of traps in the form of local optima [48].

When temperature and/or irradiation vary, the controller's capabilities in convergence speed and MPPT detection accuracy are improved by the PSO-AWDV (particle swarm optimization algorithm with adaptive weighted delay velocity) that has been proposed and applied here. The creation of the controller algorithm is the foundation for improving the PV system's performance with respect to convergence speed, stability, and accuracy.

As a means of improving PSO, a modified version called adaptive weighted delay velocity (PSO-AWDV) is proposed in reference [48]. This variant incorporates various

enhancement strategies for PSO. The following is how the new PSO's updating equations are expressed:

$$v_t^{q+1} = \mathrm{w}v_t^q + (1-\mathrm{w})v_t^{q-1} + c_1 s_1\left(P_{Best}^q - y_t^q\right) + c_2 s_2\left(G_{Best}^q - y_t^q\right) \tag{10}$$

$$y_t^{q+1} = y_t^q + v_t^{q+1} \tag{11}$$

where w is the inertia weight of velocity v_t^q and w is greater than 1; delayed velocity v_t^{q-1} having an inertia weight of $(1-w)$; the other parameter is the same as we have explained for the above Equations (4) and (5). It turns out that PSO-updating AWDV's functions are identical to those of the classical PSO with the exception of a single extra term, namely the delayed velocity and associated inertia weight.

It is important to note that the PSO-AWDV is a novel weighted delay velocity technique that can offer more power to the swarm individual particles, increasing their likelihood of escaping local entrapment and achieving the global optimum. By defining the parameter regulation rule based on this method, additional PSO variations may be created. The following part of this section introduces an innovative adaptive PSO that takes inspiration from the aforementioned factors. By evaluating the evolutionary state of the particle swarm, a new adaptive scheme is devised. This scheme utilizes the update functions from Equations (4) and (5) of the original PSO and combines them with the concept of adaptive weighted delay velocity (PSO-AWDV), incorporating insights from PSO-TVAC (particle swarm optimization with time-varying acceleration coefficients) [49]. In the PSO-TVAC approach, the acceleration coefficients of the PSO algorithm are gradually adjusted during the optimization process. The authors propose a hierarchical structure for the algorithm, where particles are organized into groups based on their fitness values and the best solutions from each group are used to update the global best solution. The utilization of time-varying acceleration coefficients helps to maintain a balance between exploration and exploitation throughout the search process. This enables the algorithm to effectively navigate away from local optima and converge towards the global optimum with improved efficiency. When the PSO-TVAC algorithm is consistent with the acceleration factors c_1 and c_2, that is

$$c_1 = (c_{1\ Initial} - c_{1\ Final}) \times \left\{\frac{q_{max} - q}{q_{max}}\right\} + c_{1\ Final} \tag{12}$$

$$c_2 = (c_{2\ Initial} - c_{2\ Final}) \left\{\frac{q_{max} - q}{q_{max}}\right\} + c_{2\ Final} \tag{13}$$

here, $c_{1\ Initial}$ and $c_{1\ Final}$ shows the initial values and final values of acceleration factor c_1, respectively; similarly $c_{2\ Initial}$ and $c_{2\ Final}$ show the initial values and final values of acceleration factor c_2, respectively; q_{max} and q indicate the maximum and current iterations in optimization. The computation and adaptive regulation of the inertia weight of velocity, denoted as w, are performed in accordance with the evolutionary state within the optimization process:

$$W = 1 - \frac{m}{1 + e^{n \times E_{st}(q)}} \tag{14}$$

where m and n are two variables that may be created to modify PSO's search efficiency; $E_{st}(q)$, is the estimation value (EV) of an evolutionary state just at k^{th} iteration which may be calculated as follows:

$$E_{st}(q) = \frac{|f_{Max}(q)| - |f_{Min}(q)|}{|f_{Max}(q)|} \tag{15}$$

where the particle's maximum and minimum fitness values at the qth iteration are denoted by f_{Max} and f_{Min}, respectively, by which PSO-AWDV is employed to track MPPT in the PV System. Figure 5 illustrates the complete configuration of a maximum power point tracking controller based on a boost converter. The flowchart of the proposed algorithm, along with the compared algorithm, is depicted in Figure 6.

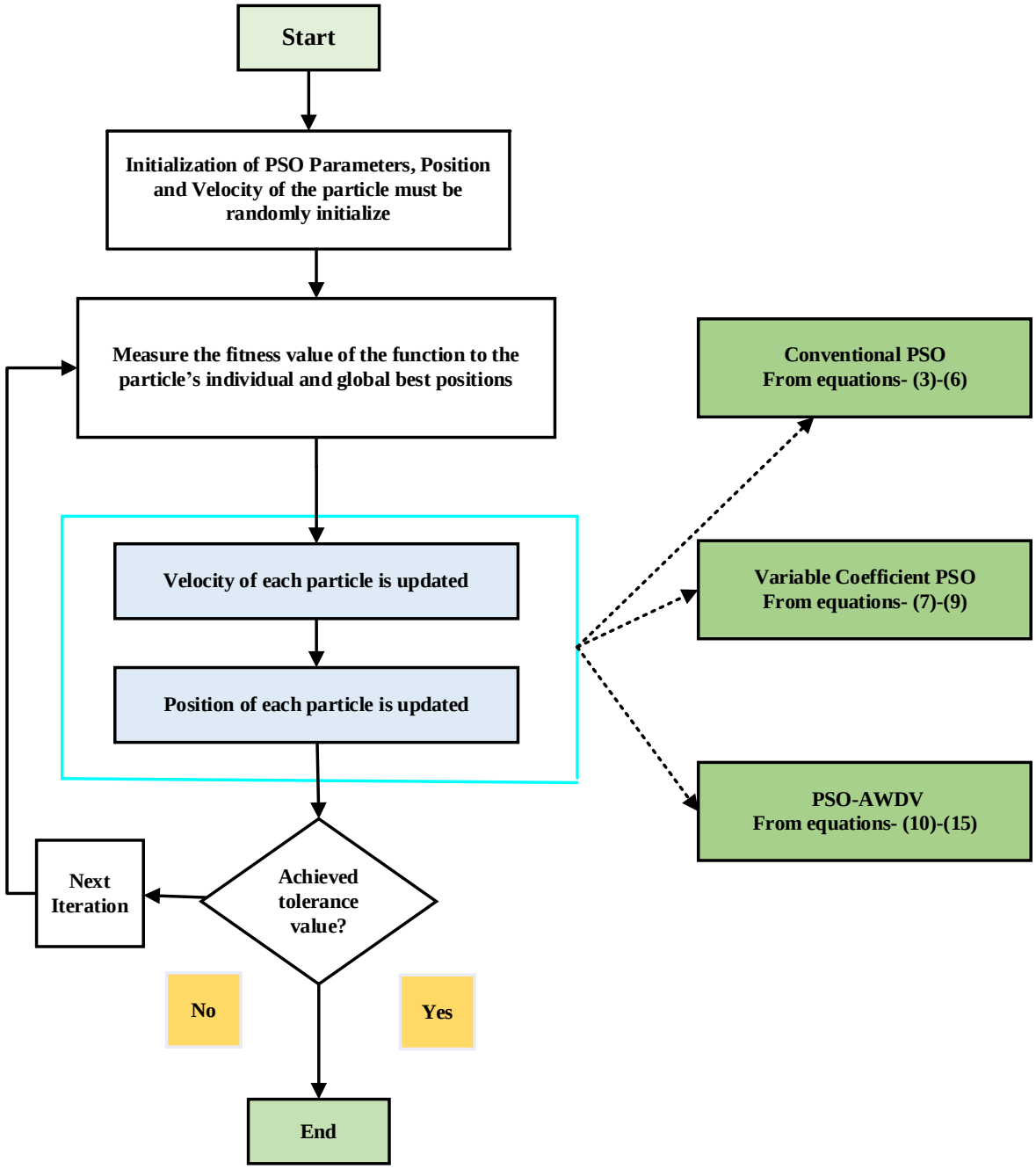


Figure 6. Flowchart for PSO-AWDV and its variants.

8. Simulation Results and Discussion

Here, in this part, we provide a comprehensive presentation of the simulation model and conduct a thorough analysis. To assess the effectiveness of the PSO-AWDV-based MPPT method, we have developed a PV system in MATLAB/Simulink®. Figure 7 visually represents this PV system, showcasing its architecture and components. In the simulation studies, a detailed description of the features of the PV array is given in Table 2. The model's name of the PV module whose parameters have been described in Table 2 is User defined. The following are also the specifications used for the DC-to-DC boost converter: 47 µF input capacitance (C_1), 470 µF output capacitance (C_2), and 1.5 mH inductance (L). A 10 Ω load resistance is connected to the pv system.

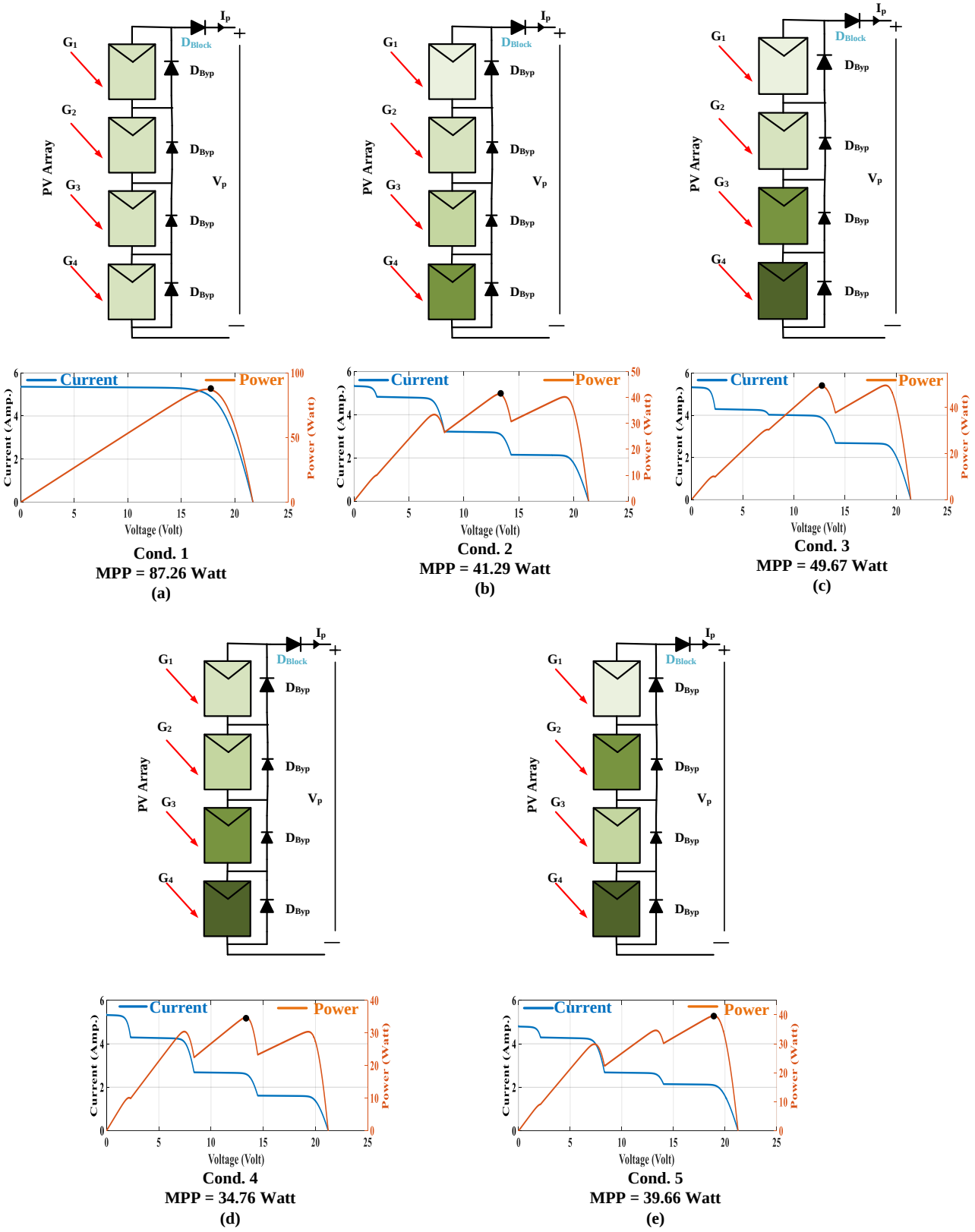


Figure 7. (**a**) Equal insolation is received by four PV modules; (**b**–**e**) four photovoltaic modules receiving uneven insolation.

Table 2. Details of the PV modules.

Parameter	Value
Number of PV modules in series	4
Short-circuit Current (I_{SC})	5.34 A
PV cells per module	72
Open-circuit Voltage (V_{OC})	5.425 V
Current at MPP (I_{MP})	5.02 A
Voltage at MPP (V_{MP})	4.35 V
Maximum Power (P_{MP})	21.837 W
Temperature Coefficient of V_{OC} in %/°C	−0.37501
Temperature Coefficient of I_{SC} in %/°C	0.075

8.1. Condition of Static Partial Shading

To contrast the effectiveness of the PSO-AWDV-based MPPT technique along with other PSO and PSO-VC methods, simulation studies were carried out using different levels of solar insolation (radiation), as depicted in Figure 7a–e. These variations in insolation values resulted in diverse shapes and peaks on the P-V characteristics. In Figure 7, the bypass diode is represented as D_{Byp}, while the blocking diode is labeled as D_{Block}. Table 3 provides a summary of the insolation settings employed in the simulated investigations.

Table 3. Different insolation values applied to the four modules of the PV array.

	Insolation (W/m^2)				
Condition	Q_1	Q_2	Q_3	Q_4	**Rated Power**
1	1000	1000	1000	1000	87.26 Watt
2	1000	900	600	400	41.29 Watt
3	1000	800	750	500	49.67 Watt
4	1000	800	500	300	34.76 Watt
5	900	800	500	400	39.69 Watt

8.1.1. Condition 1: Full Insolation

The provided simulation results in Figure 8a–c illustrate the power output and duty ratio plots for a four-module photovoltaic array operating under full insolation conditions. Three different algorithms, namely PSO, PSO-VC, and PSO-AWDV were employed for analysis. During this condition, all PV modules received a uniform irradiance of 1000 W/m^2. The outcomes reveal that PSO-AWDV exhibited superior performance in terms of tracking time and reduced fluctuations compared to the PSO and PSO-VC algorithms. PSO-AWDV effectively tracked the maximum power point (MPP) at 87.21 W with a tracking efficiency of 99.94%, achieving a convergence time of 0.32 s. On the other hand, PSO-VC with a settling time of only 1.1 s, successfully tracked the MPP but at slower pace than PSO-AWDV. PSO-VC obtained a slightly lower MPP value of 86.6 W with an efficiency of 99.24%. On the other hand, the PSO algorithm, known for its exploration and exploitation abilities, effectively tracks the MPP at 85.07 W. Nevertheless, it takes a longer time to settle compared to PSO-AWDV and PSO-VC, requiring 1.34 s. Furthermore, PSO displays greater performance even after steady-state oscillations reaching the MPP, which cause power losses and lower the MPP's efficiency by up to 97.49%. While PSO-AWDV shows a superior performance under complete insolation conditions, the fact that metaheuristic algorithms are capable of managing partial shading situations must be emphasized. In addition to their performance in optimal conditions, these algorithms need to exhibit robustness and adaptability to effectively deal with scenarios where the PV array may experience partial shading.

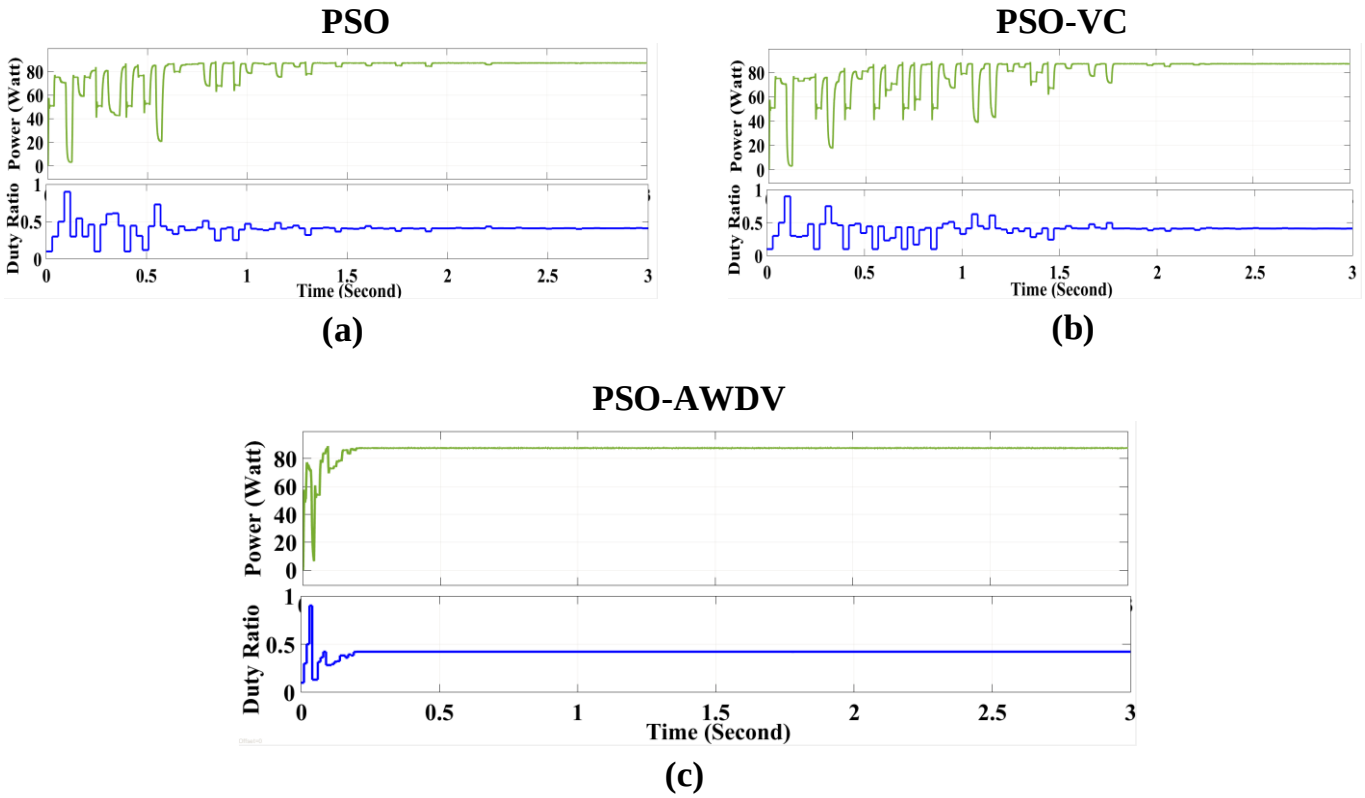


Figure 8. (**a**–**c**) Simulation results of PSO, PSO-VC, and PSO-AWDV algorithm at Condition 1.

8.1.2. Condition 2: Weak PS Condition

Under Condition 2, where PV array modules experience varying insolation values of 1000, 900, 600, and 400 W/m^2, comparison results are depicted in Figures 9a, 9b and 9c for PSO, PSO-VC and PSO-AWDV respectively. In this scenario, PSO-AWDV demonstrates successful tracking of the MPP at 41.27 W within a settling time of 0.497 s, achieving an efficiency of approximately 99.98%. PSO-VC has a settling time of 1.23 s and resulting in slightly lower MPP value of 41.16 W and an efficiency of 99.68%. On the other hand, PSO successfully tracks the MPP of 41.05 W but achieves a lower efficiency of 99.41% compared to PSO-AWDV and PSO-VC. PSO also exhibits a longer settling time of 1.331 s. Notably, PSO-AWDV outperforms the other two algorithms with significant improvements in settling time. The outcomes also show that PSO-AWDV achieves greater efficiency in comparison to PSO and PSO-VC algorithms and exhibits a notable increase in within convergence speed.

8.1.3. Condition 3: Strong PS Condition

In Condition 3, the results are compared using Figure 10a–c where one panel receives 1000 W/m^2 while the remaining panels receive 800 W/m^2, 750 W/m^2, and 500 W/m^2 respectively. In this strong PS condition, PSO-AWDV successfully track the MPP at 49.63 W having a settling time of 0.6004 s and an efficiency of approximately 99.91%. On the other hand, PSO-VC takes a longer tracking time of 2.149 s and settles at 49.29 W with a 99.23% efficiency, which is a somewhat lower value. PSO successfully tracks the MPP of 49.15 W, but with a lower efficiency of 98.95% having a tracking time of 2.198 s compared to another algorithm. PSO-AWDV exhibits fewer fluctuations during the search for the MPP compared to PSO-VC and PSO, leading to significant reduction in power losses.

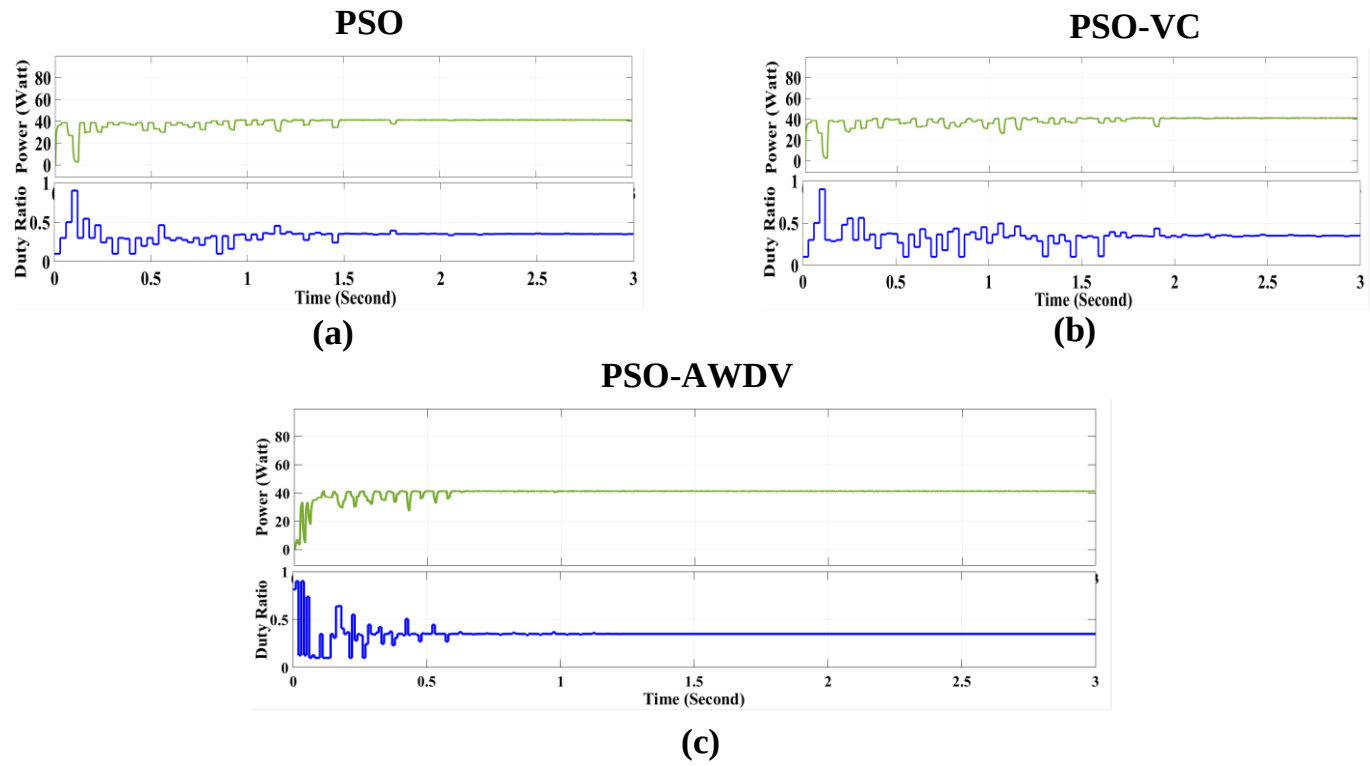


Figure 9. (**a**–**c**) Simulation results of PSO, PSO-VC and PSO-AWDV algorithm at Condition 2.

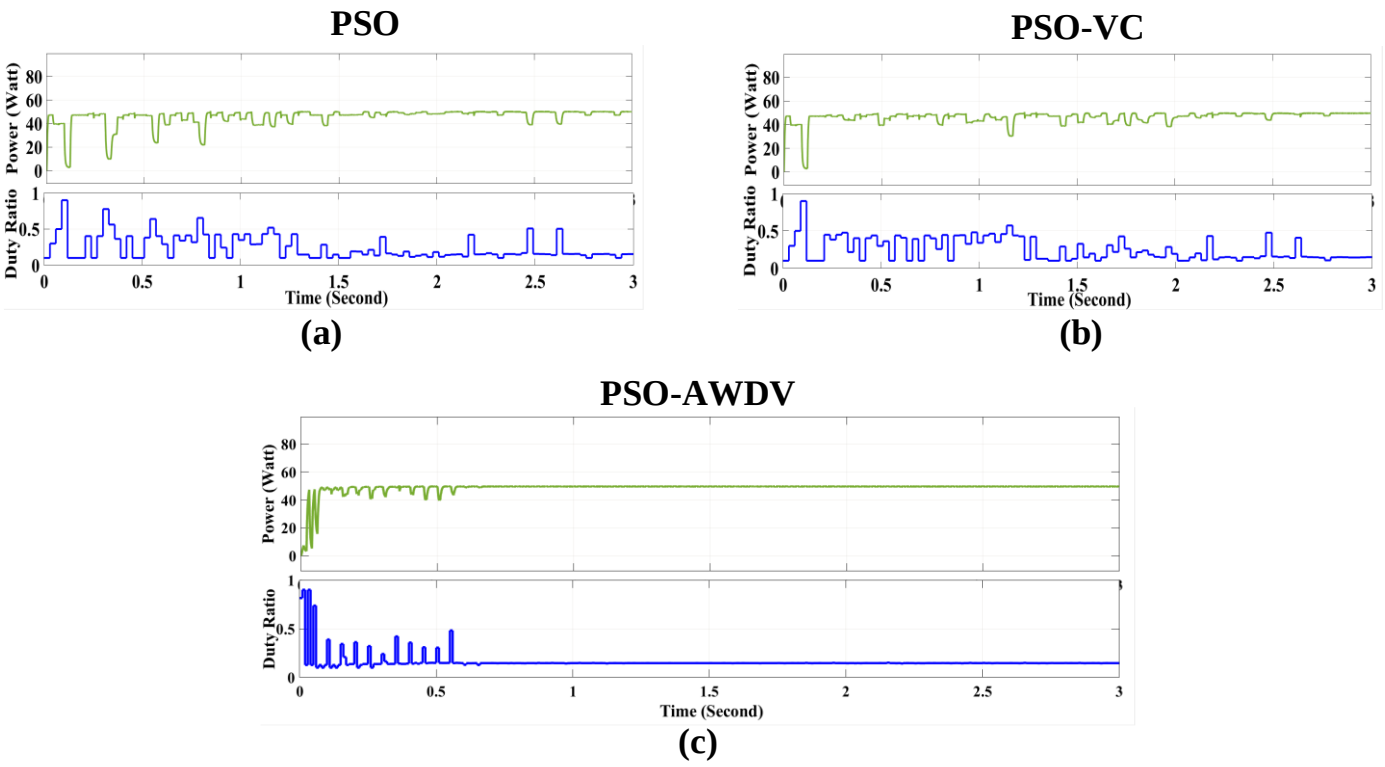


Figure 10. (**a**–**c**) Simulation results of PSO, PSO-VC and PSO-AWDV algorithm at Condition 3.

8.1.4. Condition 4: Strong PS Condition

In Condition 4, we analyzed the performance by comparing the results in Figure 11a–c. In this scenario, one panel received a solar irradiance of 1000 W/m^2, while the remaining panels received 800 W/m^2, 500 W/m^2, and 400 W/m^2, respectively. Under these conditions, PSO-AWDV demonstrated remarkable success in tracking the maximum power point (MPP), achieving a precise MPP of 34.7 W within a quick settling time of 0.4711 s. Furthermore, it exhibited an impressive efficiency of approximately 99.94%. In contrast, the PSO-VC algorithm took a longer time to track the MPP, requiring 1.853 s, and settled at slightly lower value of 34.62 W. Its efficiency was also slightly lower, at 99.71%. The standard PSO algorithm managed to track the MPP at 34.42 W, but it exhibited a lower efficiency of 99.135% and took 1.786 s to do so, making it less efficient compared to the other algorithm variants. Notably, PSO-AWDV displayed fewer fluctuations during its search for the MPP compared to PSO-VC and the standard PSO algorithm. This reduction in fluctuations translated into a significant reduction in power losses, highlighting its superiority in this specific condition.

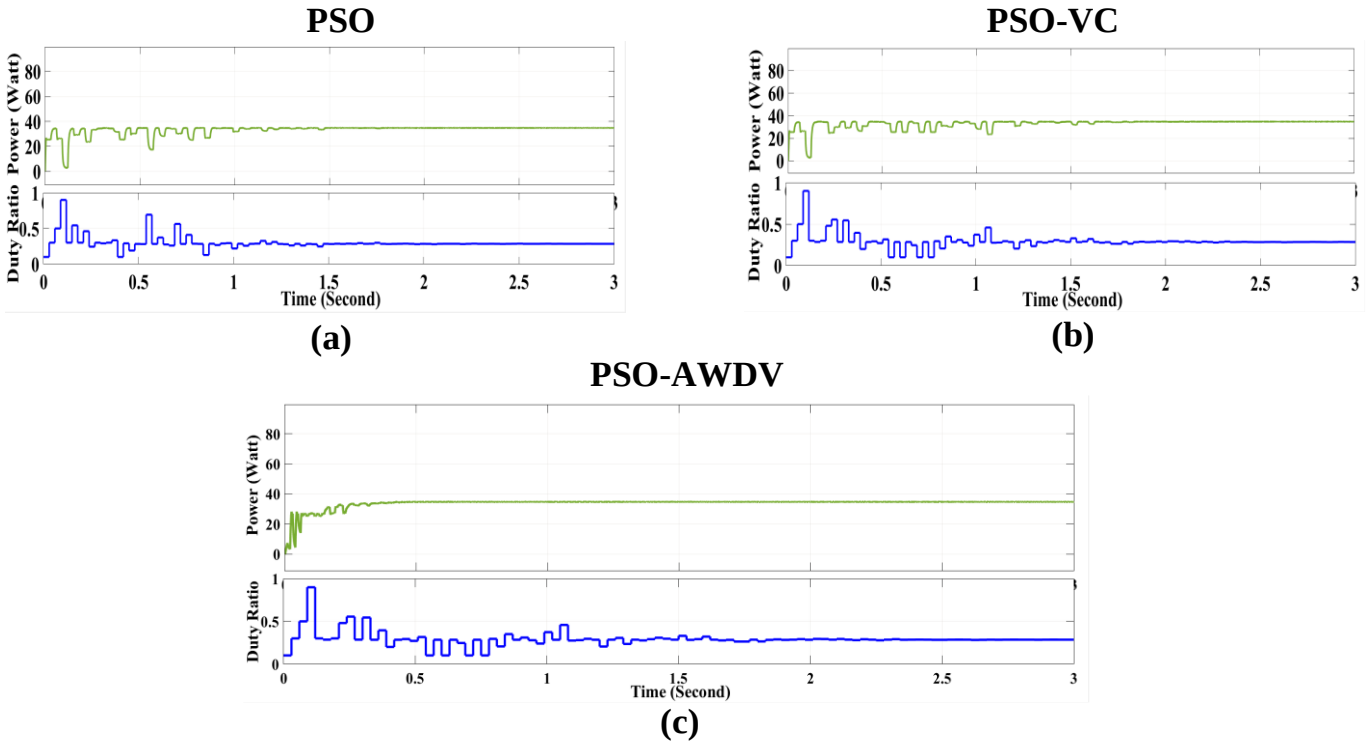


Figure 11. (**a**–**c**) Simulation results of PSO, PSO-VC and PSO-AWDV algorithm at Condition 4.

8.1.5. Condition 5: Strong PS Condition

In Condition 5, we conducted a comparative analysis of the outcomes depicted in Figure 12a–c. This analysis involved varying solar irradiance levels, with one panel receiving 900 W/m^2, while the other panels received 800 W/m^2, 500 W/m^2, and 400 W/m^2, respectively. Under these conditions, PSO-AWDV demonstrated exceptional performance in tracking the maximum power point (MPP). It precisely tracked the MPP at 38.74 W, achieving this result swiftly with a settling time of 0.2611 s and an efficiency of approximately 97.60%. In contrast, the PSO-VC algorithm took less duration to track the MPP as compared to the PSO-AWDV, that is 0.4252 s to settle at a lower value of 36.99 W, having an efficiency of 93.197%. The standard PSO algorithm managed to track the MPP at 36.81 W, but it exhibited a lower efficiency of 92.74% and had a tracking time of 1.153 s compared to the other algorithms. As for the simulation results of PSO and PSO-VC algorithms, noticeable variations were observed. Due to these fluctuations significant power dips occurred, resulting in increased power losses. Additionally, the convergence decision after tracking

the MPP during changes in insolation was slow, leading to undesirable fluctuations, unnecessary power dips, and losses. In contrast, the PSO-AWDV algorithm demonstrated a rapid convergence rate and maintained a consistent plot size while settling at the MPP. Notably, the suggested approach demonstrated quick and complete convergence once the MPP was located. As a result, it effectively maintained power output even in complex PS scenarios without deviating from its usual performance. This achievement was made possible through the algorithm's intelligent search space management, ensuring reliability, efficiency, and meeting the required criteria. Figure 13 provides a concise comparative summary of all PSO-AWDV, PSO-VC, and PSO algorithms, focusing on their tracking time, MPP tracking capabilities, and their efficiency.

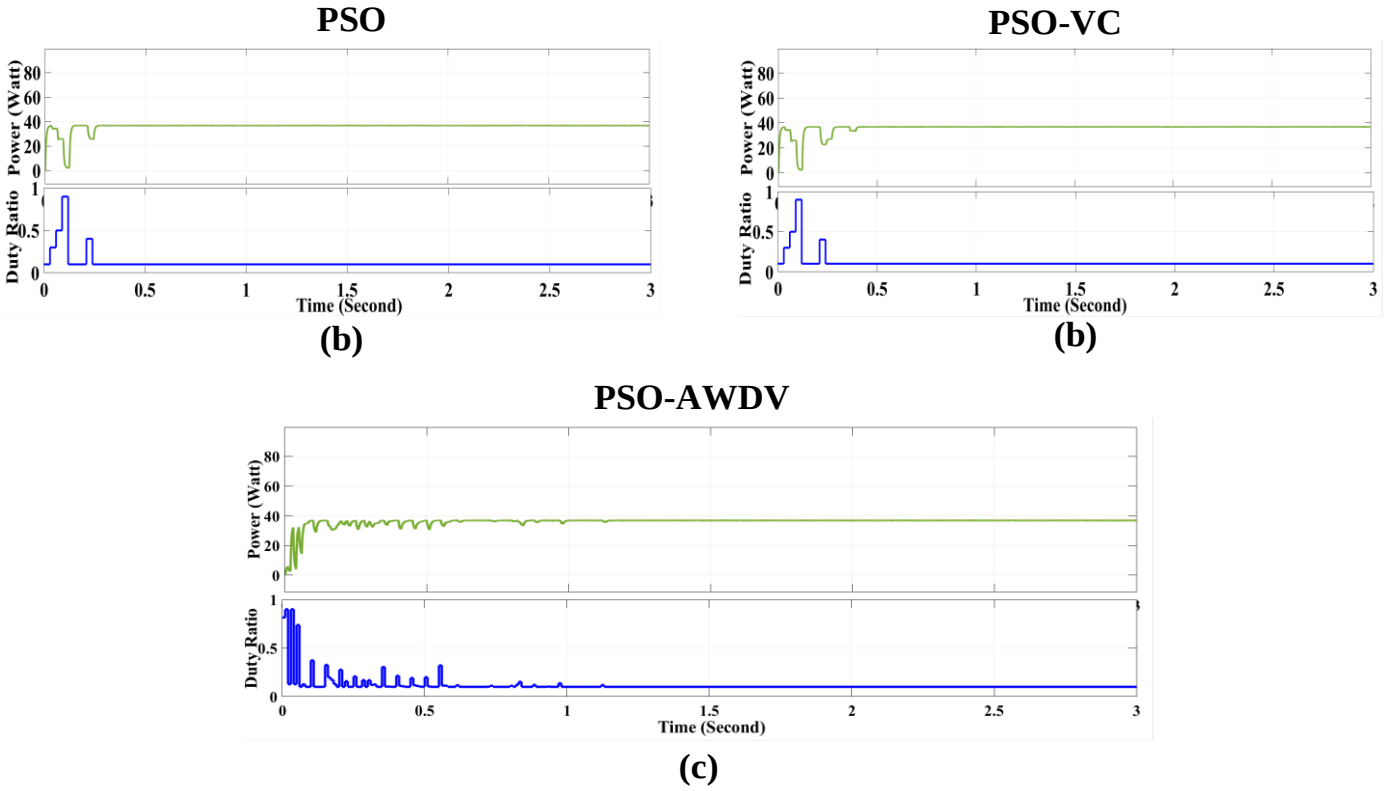


Figure 12. (**a**–**c**) Simulation results of PSO, PSO-VC and PSO-AWDV algorithm at Condition 5.

8.2. Dynamic Partial Shading Condition

The performance of the PSO-AWDV-based MPPT approach is evaluated in the presence of dynamic changes in insolation circumstances in order to improve its superiority, resilience, reliability, and efficiency. Testing in dynamic conditions is essential because PV arrays in real-world situations experience different degrees of shade as a result of environmental changes. Therefore, this study includes a gradual change in insolation. On the PV string, Figure 14 depicts abrupt changes in incident insolation levels. The initial uniform distribution that was seen in Condition 1 is altered to another condition after 1 s with insolation values of 1000 W/m^2, 900 W/m^2, 600 W/m^2, and 400 W/m^2, which is a mild PS situation. Then, as in Condition 3, this is further altered to a partial shade condition with an insolation level of 900 W/m^2, 800 W/m^2, 500 W/m^2, and 400 W/m^2. At last, the insolation level changes after 1 s from the third insolation level to the fourth insolation level which is 1000 W/m^2, 800 W/m^2, 500 W/m^2, and 300 W/m^2. These changes in the insolation level take place after every 1 s. The algorithm must restart itself in response to these changes in insolation in order to monitor the MPP more quickly. At a uniform insolation level, PSO-AWDV converges in 0.3 s and produces a maximum power of 86.1 W, yielding an efficiency of 99.69%. The PV array's insolation levels abruptly switch from insolation level

1 to insolation level 2. At this insolation level, PSO-AWDV tracked an MPP of 39.22 W in 1.23 s, having an efficiency of 99.98%. At the third insolation level, the time taken to track the MPP of 39.42 W is 2.172 s. At the last insolation level, it tracked the MPP of 37.88 W, and tracking this maximum power point took 3.25 s. According to the simulation findings, the suggested PSO-AWDV algorithm is extremely sensitive to changes in shaded patterns. The results also imply that the proposed PSO-AWDV may follow GMPP efficiently over a short time and exhibit minimal oscillations during transients.

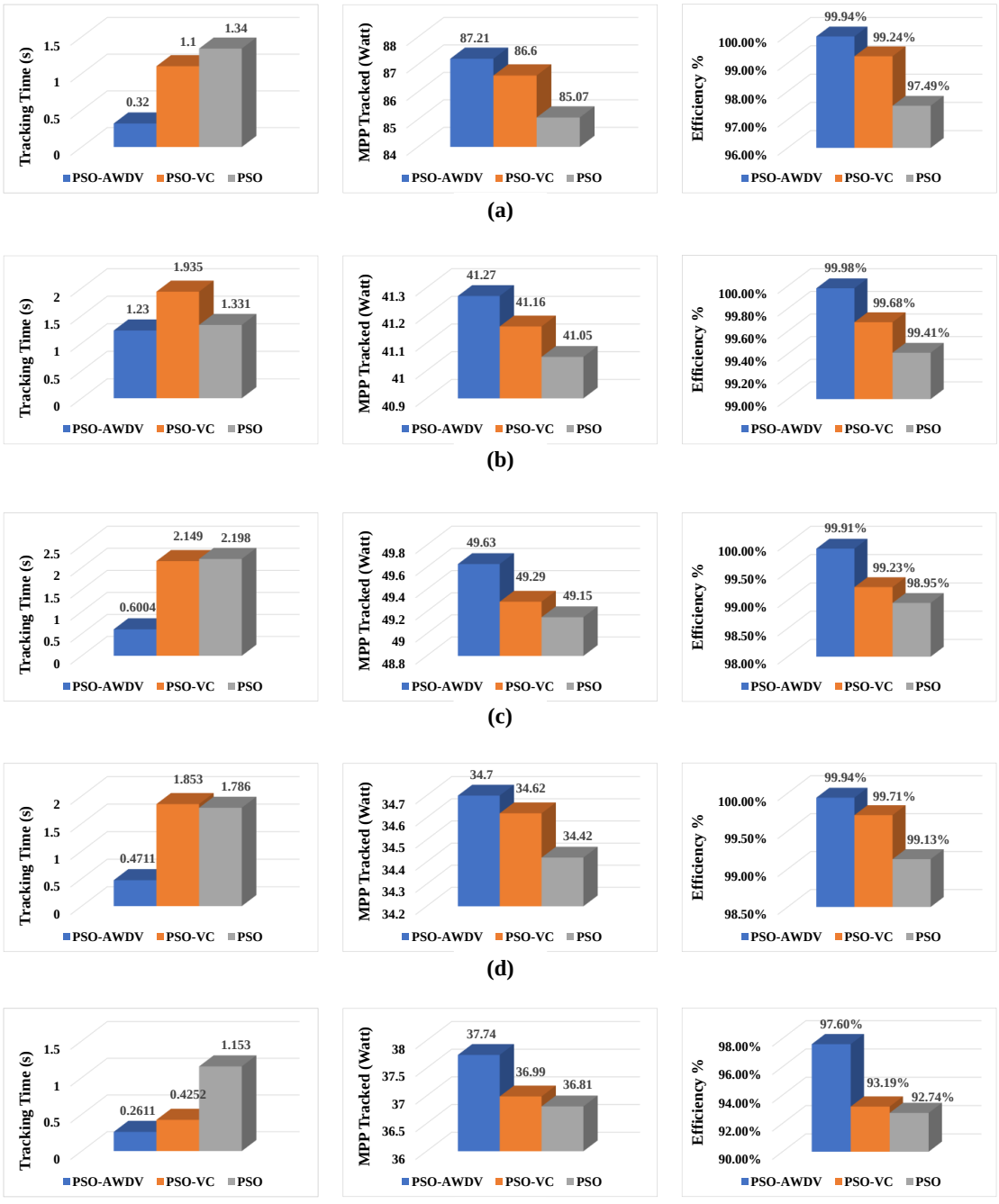


Figure 13. Comparison charts of PSO-AWDV, PSO-VC, and PSO for tracking time, MPP tracked, and efficiency for (**a**) Cond. 1, (**b**) Cond. 2, (**c**) Cond. 3, (**d**) Cond. 4, and (**e**) Cond. 5.

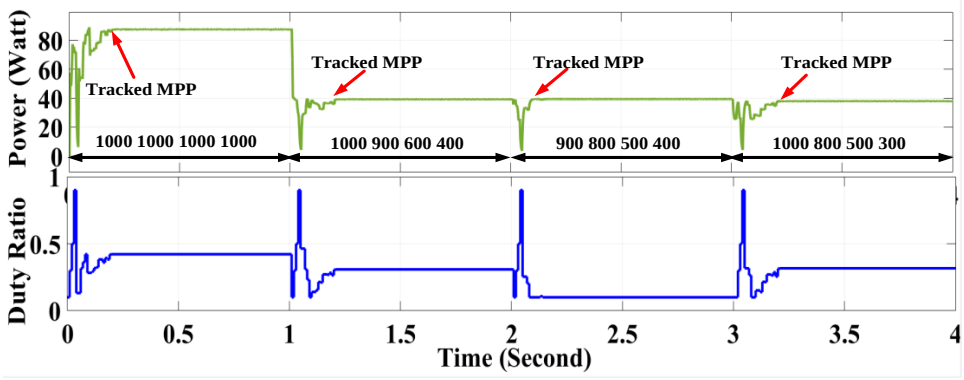


Figure 14. PSO-AWDV-based MPPT simulation output for dynamic insolation circumstances.

8.3. Effect of Load Change

In this section, the simulation results demonstrate the reliability and robustness of the proposed PSO-AWDV-based MPPT method through load variation. Figure 15 illustrates this variation at constant irradiance of 1000, 900, 750, and 400 W/m^2 on the four modules of the PV array. Initially, a 10 Ω load is applied, and after 1 s, the load transitions to 5 Ω. The results indicate that with a 10 Ω load, the maximum power tracked is 49.94 W within a 0.23-s timeframe. After the load switches to 5 Ω, the maximum power tracked becomes 49.84 W within a 0.16-s interval.

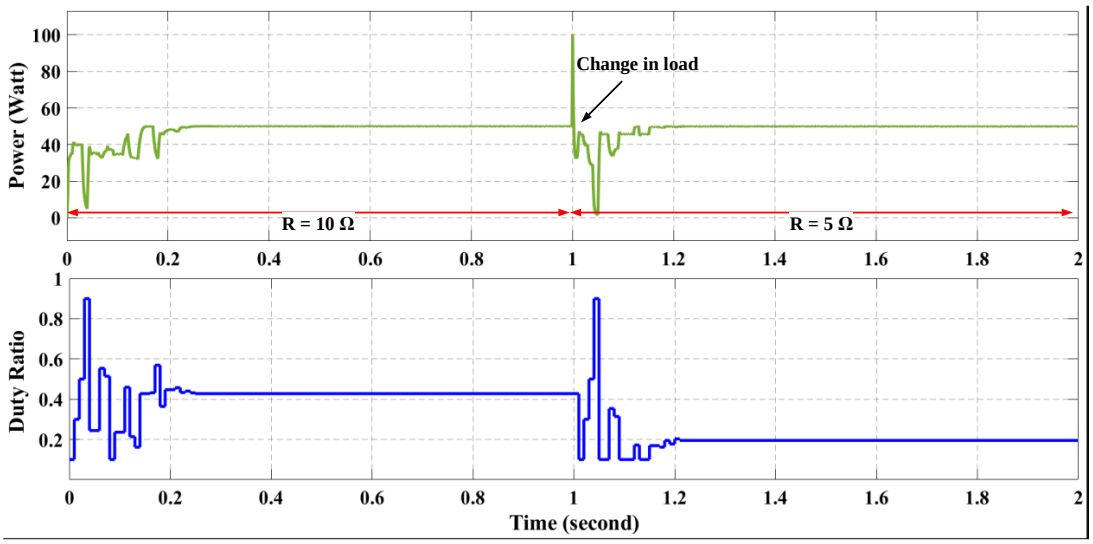


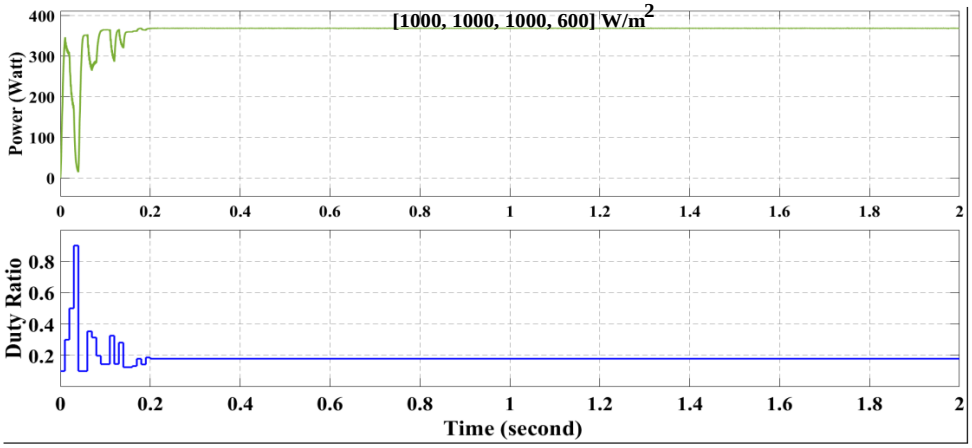
Figure 15. PSO-AWDV-based MPPT simulation output for change in load from 5 Ω to 10 Ω.

In summary, altering the load leads to only minor variations in the maximum power tracked. These variations are attributed to changes in the size and frequency of power fluctuations during the initial iterations, as well as an increase in tracking time. Nonetheless, these variations are minimal and do not result in significant power losses. Consequently, the proposed algorithm exhibits a stable performance even when the load is modified.

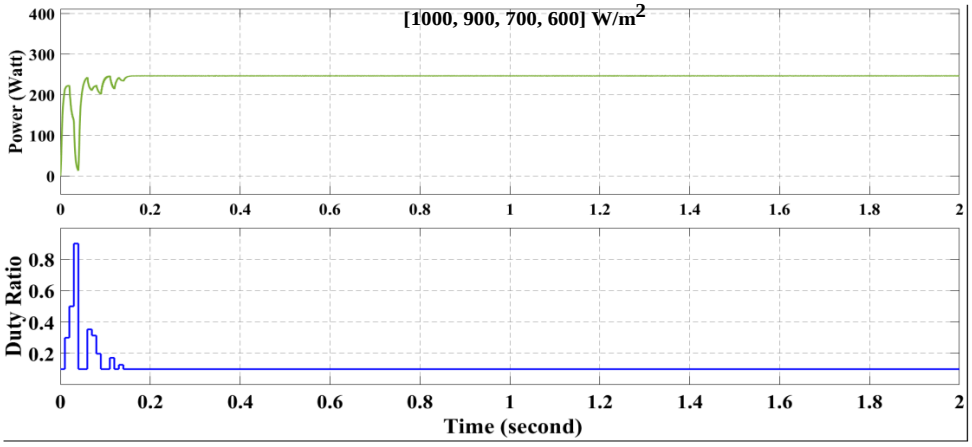
8.4. Effect of PV Module Change

In this subsection, validation of the proposed PSO-AWDV-based MPPT method is carried out using the commercially available PV module, Inventec Energy IECS-6P66-125, within the MATLAB R2019a software environment. Figure 16 illustrates the MPP tracking capability of the PSO-AWDV algorithm, showcasing the curves corresponding to the data in Table 4. Specifically, Figure 16a,b present the curves for irradiance scenarios 1 (1000, 1000, 1000, 600 W/m^2) and 2 (1000, 900, 700, 600 W/m^2), respectively. From Figure 16a, we

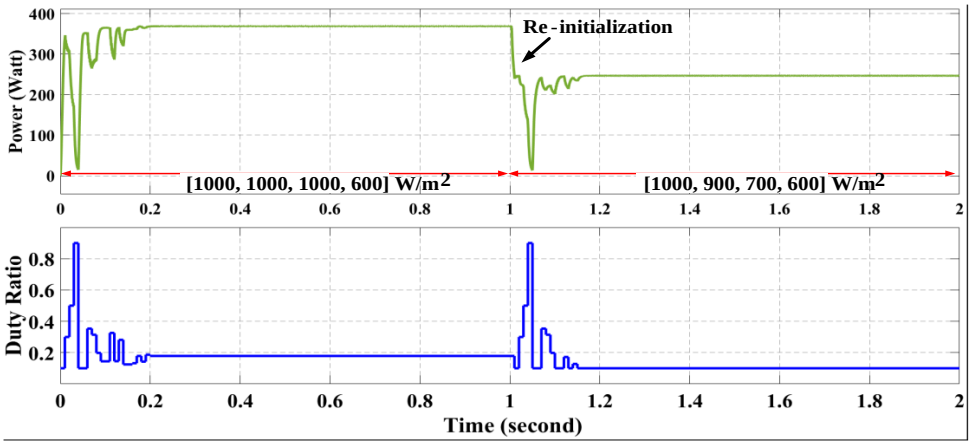
observe that the algorithm achieves a maximum power of 369.8 W with a convergence time of 0.2 s. In Figure 16b, the maximum power tracked is 247.1 W, with a convergence time of 0.16 s.



(a)



(b)



(c)

Figure 16. PSO-AWDV-based MPPT simulation output using Inventec Energy IECS-6P66-125 PV module for (**a**) irradiance scenario 1; (**b**) scenario 2; and (**c**) when the irradiance is dynamically changed from scenario 1 to scenario 2.

Table 4. Specifications of Inventec Energy IECS-6P66-125 module.

Parameter	Value
The temperature at standard test condition (T_{STC})	298.15 K
Standard irradiance for testing purposes (G_{STC})	1000 W/m^2
Number of PV modules linked in series	4
PV cells per module	36
Short-circuit Current (I_{SC})	7.91 Amperes
Open-circuit Voltage (V_{OC})	21.6 Volts
The current at MPP (I_{MP})	7.4 Amperes
The voltage at MPP (V_{MP})	16.93 Volts
Maximum Power (P_{MP})	125.282 Watts
Temperature Coefficient of V_{OC} in %/°C	−0.35602
Temperature Coefficient of I_{SC} in %/°C	0.07

To further assess the practicality of the proposed method, the PV output curve is presented in Figure 16c when the irradiance condition shifts from scenario 1 (1000, 1000, 1000, 600 W/m^2) to scenario 2 (1000, 900, 700, 600 W/m^2) after a 1-s interval. Notably, the tracking time and system efficiency remain unaffected in this scenario, emphasizing the stability of the algorithm.

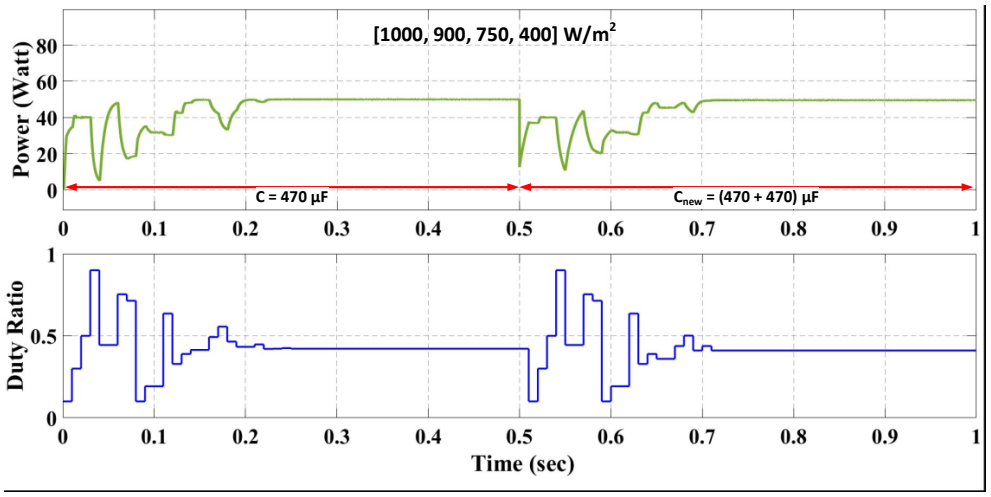
While it is important to acknowledge that there is no absolute guarantee of the optimal performance of any algorithm in all environments, the proposed algorithm demonstrates remarkable stability and versatility after extensive testing with various module ratings, shading scenarios, and changing irradiance conditions. This consistency instils confidence in its suitability for industrial applications. In particular, the algorithm's robust performance across different module configurations implies its utility when modifying the rating of the array. For instance, when adjusting the rating of an array, the existing MPP tracker equipped with the PSO-AWDV algorithm can be retained, eliminating the need for purchasing a new tracker. Additionally, its resilience following a module rating change suggests that, even years later when a new PV array is installed, the tracker incorporating the PSO-AWDV algorithm will continue to deliver stable performance, obviating the need for replacement.

8.5. Performance Evaluation Test for Robustness against Converter Parametric Uncertainties

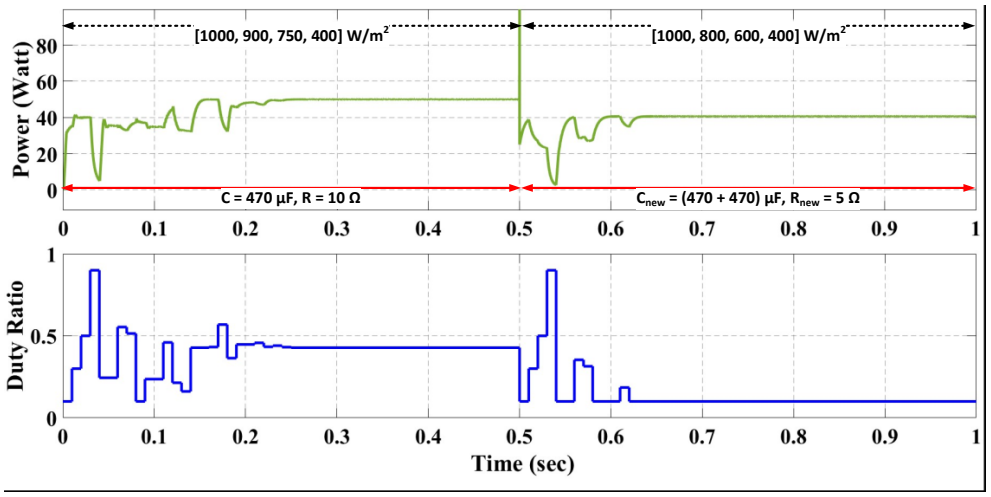
The study presents an examination of the robustness and superior performance of the PSO-AWDV-based MPPT method, particularly in the context of variations in the parameters of the DC–DC converter. To rigorously evaluate this method, uncertainties are introduced in the value of the output capacitor (C_2) of the DC–DC converter.

As depicted in Figure 17a, C_2 is incrementally increased by ΔC = 470 µF after 0.5 s, resulting in $C_{new} = C_2 + \Delta C$, while maintaining constant irradiance levels at (1000, 900, 750, 400) W/m^2. Initially, the system tracked an output PV power of 50.2 W in 0.22 s only. Subsequently, even with the alteration in the capacitance of the PV plant, the PV power tracked remained impressively high at 49.68 W, achieved in just 0.2 s. Notably, this slight deviation in the output power did not exhibit any discernible impact on the convergence time of the algorithm.

Furthermore, Figure 17b portrays the PV array output power under varying conditions, including changes in the DC–DC converter parameters, irradiance levels, and load. Specifically, after 0.5 s, C_2 was increased by ΔC = 470 µF, and the load was adjusted from 10 Ω to 5 Ω, while irradiance levels shifted from (1000, 900, 750, 400) W/m^2 to (1000, 800, 600, 400) W/m^2. In this scenario, the initial output PV power tracked stood at an impressive 50.26 W, attained within 0.22 s. Subsequently, despite the considerable changes in system conditions, the final output PV power settled at 40.68 W, impressively accomplished within only 0.12 s.



(a)



(b)

Figure 17. PV array output power when (**a**) boost converter capacitance is varied keeping the irradiance the same, (**b**) boost converter capacitance and load are varied under dynamic irradiance conditions.

These observations unequivocally highlight the remarkable resilience and agility of the proposed PSO-AWDV controller technique. It consistently attains steady-state performance swiftly and exhibits unwavering robustness in MPPT tracking.

9. Hardware-In-The-Loop (HIL) Implementations of PSO-AWDV Algorithm

This section validates the PSO-AWDV algorithm by evaluating its real-time MPP tracking performance and benchmarking it against other MPPT techniques. To determine the usefulness and superiority of the suggested strategy, a thorough comparison is performed with different MPPT algorithms that are already in use. To evaluate the performance of MPPT algorithm, the Typhoon hardware-in-the-loop (HIL) 402 emulator is utilized. In this evaluation, a DC-to-DC boost converter acts as an intermediate component between the PV array and the load, facilitating the implementation of the MPPT technique. The boost converter's duty ratio is carefully adjusted to maximize power output by altering the current and voltage at the output while taking the current level of solar intensity into consideration. In the context of the PSO-AWDV algorithm, this duty ratio can be considered as one of the parameters that is fine-tuned for improved performance. The real-time simulation outcomes are acquired by employing the Typhoon HIL device. To incorporate the PSO-AWDV

algorithm, it is integrated into the advanced C function model of the Typhoon HIL block, functioning in a way analogous to the microcontroller. In every iteration, power values are initially computed for four distinct duty ratio values. Subsequently, the PSO-AWDV equations are employed to update all four duty ratio values. This iterative process persists until the simulation runtime is completed.

By contrasting the proposed algorithm with the PSO as well as PSO-VC, its performance is assessed in terms of convergence time towards the global maximum power point, as well as the quantity and intensity of fluctuations observed after algorithm initialization. The size and ratings of the PV module as well as the DC-to-DC boost converter remain the same as before.

9.1. Condition of Static Partial Shading

To illustrate the efficacy of the suggested algorithm, the P-V curves of different PS circumstances listed in Table 5 are used, as seen in Figure 18. These conditions are further elaborated in subsequent subsections to provide detailed explanations.

Table 5. Different insolation values applied to the four modules of the PV array.

	Insolation (W/m^2)				
Condition	Q_1	Q_2	Q_3	Q_4	**Rated Power**
1	1000	1000	1000	1000	87.26 Watt
2	1000	1000	1000	600	61.45 Watt
3	1000	700	400	300	30.04 Watt
4	1000	800	650	400	43.98 Watt

9.1.1. Condition 1

In our study, we consider Condition 1, which represents a straightforward scenario where all PV modules receive equal amount of insolation at 1000 W/m^2. The convergence characteristics of the PSO, PSO-VC and PSO-AWDV algorithms are analyzed through Figure 19a, Figure 19b, and Figure 19c, respectively. Figure 19c reveals that the PSO-AWDV algorithm achieves convergence swiftly at a greater power value of 86.10 W, having a efficiency of 99.69%, with a tracking time of 3.6 s. Figure 19b depicts the convergence behavior of the PSO-VC algorithm, which settles at an effective convergence of 98.77% with an MPP of 85.40 W after approximately 6.0 s. Figure 19a displays the convergence behavior of the PSO algorithm, which achieves convergence with a settling time of 5.2 s, yielding a convergence efficiency of 98.06% and an MPP of 84.58 W. Furthermore, despite the initial ability of the algorithm to track the maximum power point (MPP) at an early stage, subsequent fluctuations were observed before achieving final convergence. It is crucial to keep in mind that the convergence rates seen in the hardware-in-the-loop (HIL) findings could not match those attained through simulation under the same insolation patterns. This disparity is due to the Typhoon HIL platform's real-time analytical capabilities and the stochastic character of the used metaheuristic algorithms. Consequently, different convergence rates may be seen in the simulation data.

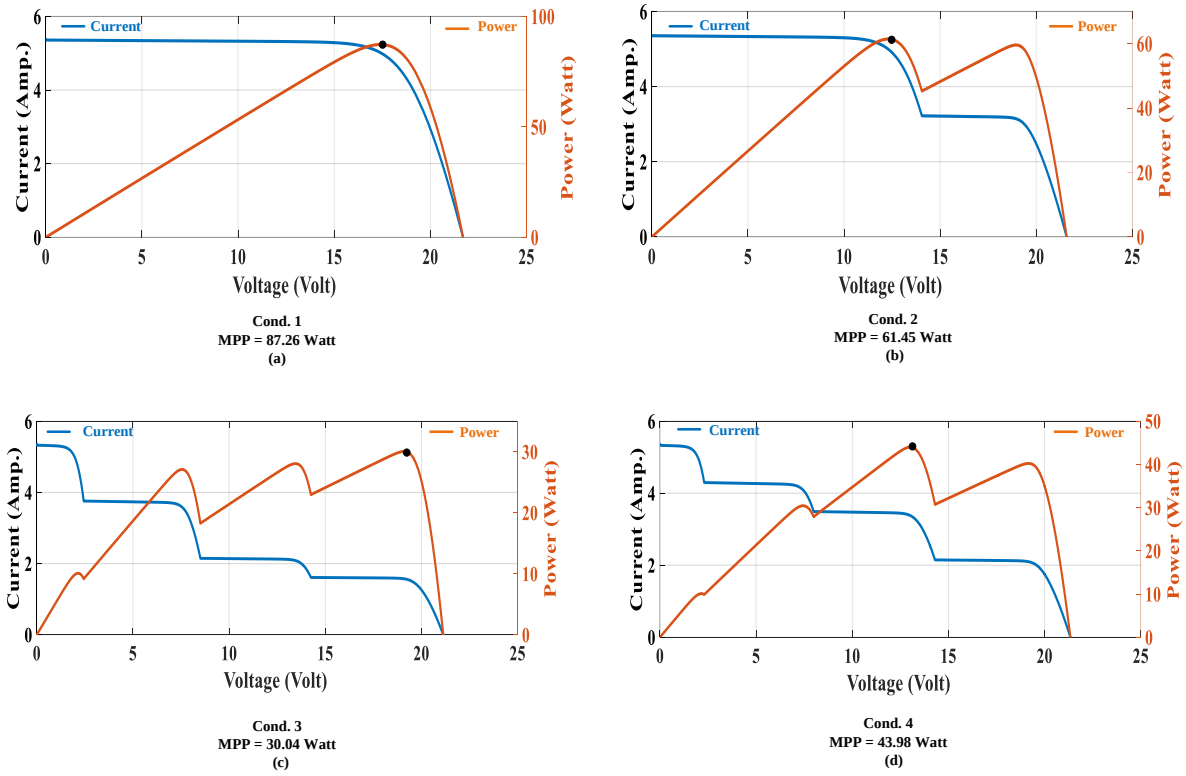


Figure 18. Power vs. voltage and current vs. voltage characteristics at (**a**) Cond. 1, (**b**) Cond. 2, (**c**) Cond. 3 and (**d**) Cond. 4 of the PV array.

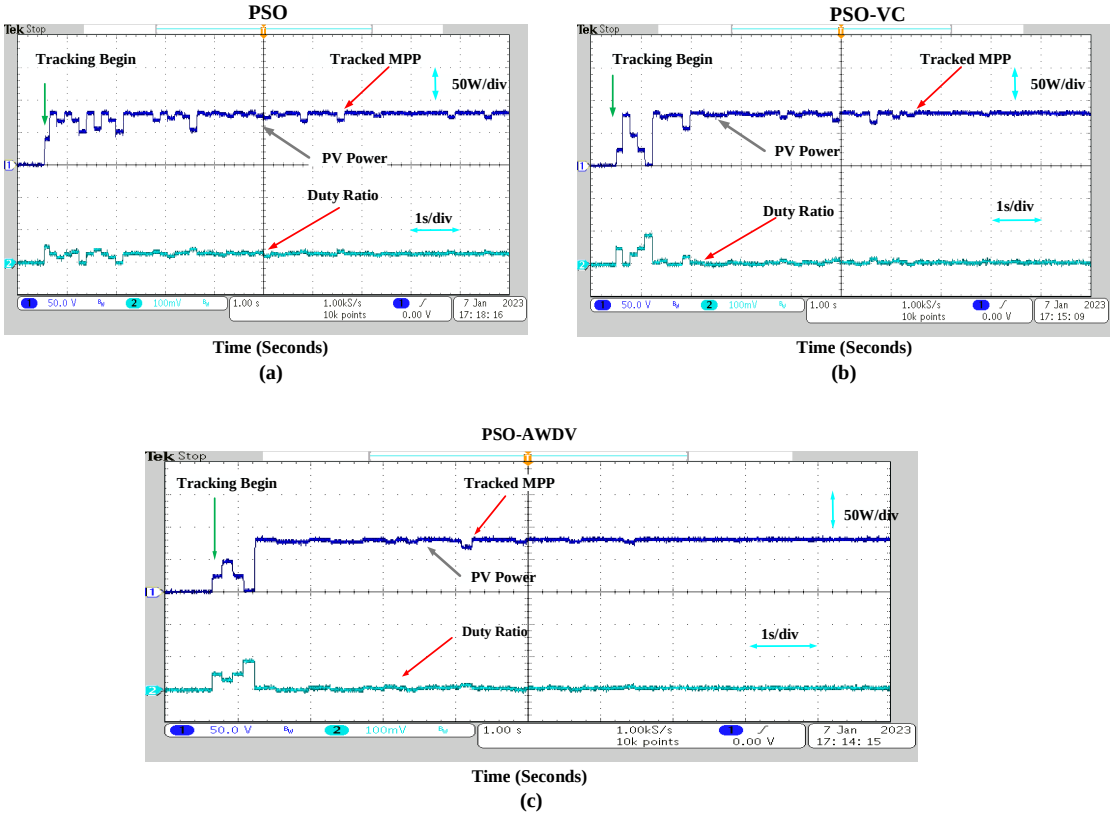


Figure 19. HIL results of (**a**) PSO, (**b**) PSO-VC and (**c**) PSO-AWDV-based MPPT at Condition 1.

9.1.2. Condition 2

Condition 2 introduces an arrangement where one module receives shaded insolation of 600 W/m^2, while the remaining three modules receive full insolation at 1000 W/m^2. The corresponding HIL results of the PSO, PSO-VC, and PSO-AWDV algorithms are presented in Figure 20a, Figure 20b, and Figure 20c, respectively. The PSO-AWDV algorithm successfully reaches the maximum power point (MPP) at 61.3 W, demonstrating a rapid convergence rate of 0.4 s and exhibiting negligible significant oscillations. These findings highlight the algorithm's capability to keep solutions within a confined search space. Furthermore, the PSO-AWDV algorithm achieves a notable efficiency of 99.75%. Similarly, the PSO-VC algorithm attains the MPP at 60.0 W, albeit with a slightly longer tracking time of 2.2 s. However, the efficiency obtained by PSO-VC is marginally lower than that of PSO-AWDV, measuring at 97.64%. Conversely, the PSO algorithm converges to the MPP at 58.2 W but exhibits a lower tracking efficiency of 94.7%. The marginal decrease in efficiency observed in the PSO-VC algorithm, in comparison to PSO, can be attributed to the presence of larger fluctuations, which contribute to amplified power losses. Additionally, monitoring the PSO time algorithm is higher than that of PSO-AWDV and PSO-VC that is 5 s.

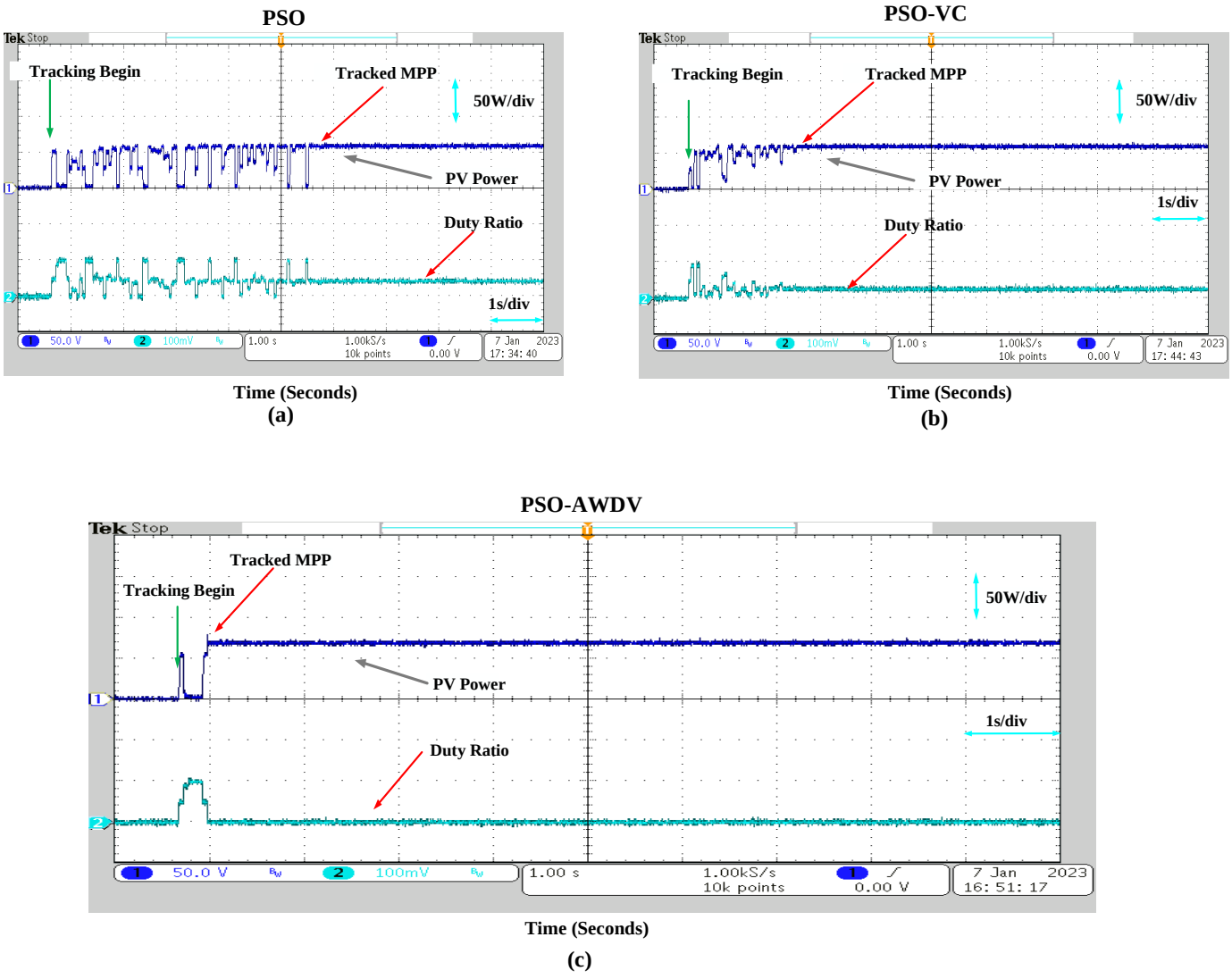


Figure 20. HIL results of (**a**) PSO, (**b**) PSO-VC and (**c**) PSO-AWDV-based MPPT at Condition 2.

9.1.3. Condition 3

In the case of Condition 3, this is characterized by a distinct shading pattern with varying insolation levels of 1000 W/m^2, 700 W/m^2, 400 W/m^2, and 300 W/m^2 across the PV string. The tracked power and duty cycle plots for the PSO, PSO-VC, and PSO-AWDV algorithms, respectively, are shown in Figure 21a–c at Condition 3. The PSO-AWDV algorithm exhibits outstanding performance, rapidly converging to the MPP of 30.0 W with a tracking time of 0.2 s, accompanied by a remarkable power generation efficiency of 99.86%. However, the PSO-VC and PSO algorithms, while successfully reaching the MPP, demonstrate longer convergence times and more pronounced oscillations. PSO-VC achieves a power of 29.9 W in 1.4 s, albeit with a slightly lower tracking efficiency of 99.53% compared to PSO-AWDV. PSO, with a 1.8 s convergence period, settles at 29.6 W and a tracking accuracy of 98.53%. The settling times of PSO-VC and PSO remain unimproved, despite the fact that all algorithms perform well in terms of power generation efficiency under this scenario. In addition, PSO and PSO-VC have slightly larger power losses as a result of their extended convergence times and a higher frequency of large-sized oscillations.

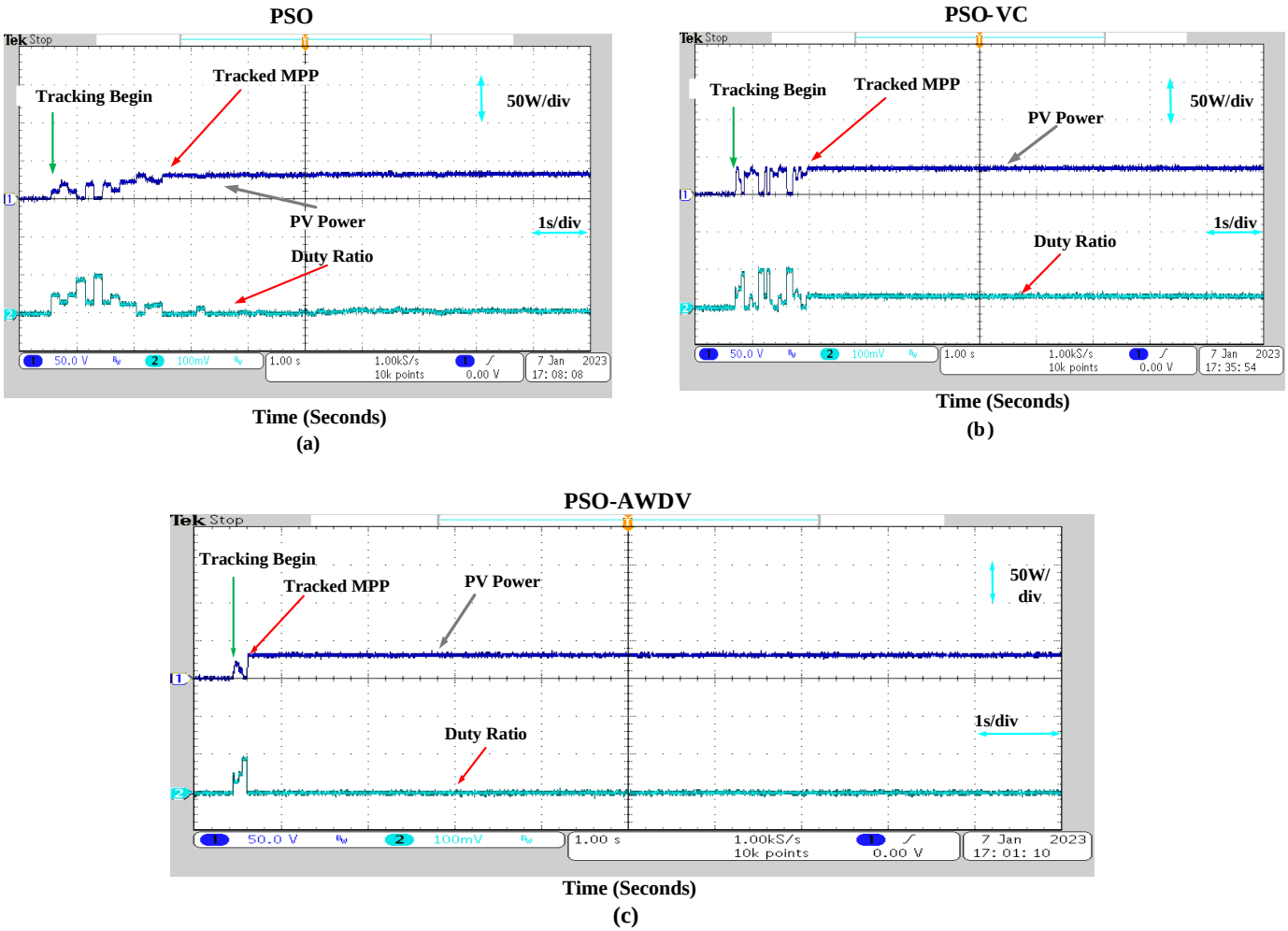


Figure 21. HIL results of (**a**) PSO, (**b**) PSO-VC and (**c**) PSO-AWDV-based MPPT at Condition 3.

9.1.4. Condition 4

In this particular case, three of the four PV modules on the PV (photovoltaic) array are partially shaded, resulting in a partial shading (PS) situation. The shaded panels' respective insolation levels are 800 W/m^2, 650 W/m^2, and 400 W/m^2. The results of the study as shown in Figure 22a, Figure 22b, and Figure 22c of PSO, PSO-VC, and PSO-AWDV, respectively, are as follows: PSO-AWDV achieved settling of the MPP in 1.6 s

having a tracking efficiency of 99.36%. Efficiency was increased as a result of the final convergence occurring more quickly at the MPP of 43.7 W. PSO-VC had a slightly weaker efficiency of 97.77% than PSO-AWDV, tracking an MPP of 43.0 W in 3.6 s. PSO, under this PS condition, had a convergence time of 4.8 s with the least tracking efficiency of 95.72 Due to larger oscillations and increased power losses, it only reached a lower MPP of 42.10 W. However, in terms of tracking effectiveness and settling time, PSO-AWDV and PSO surpassed PSO-VC and PSO.

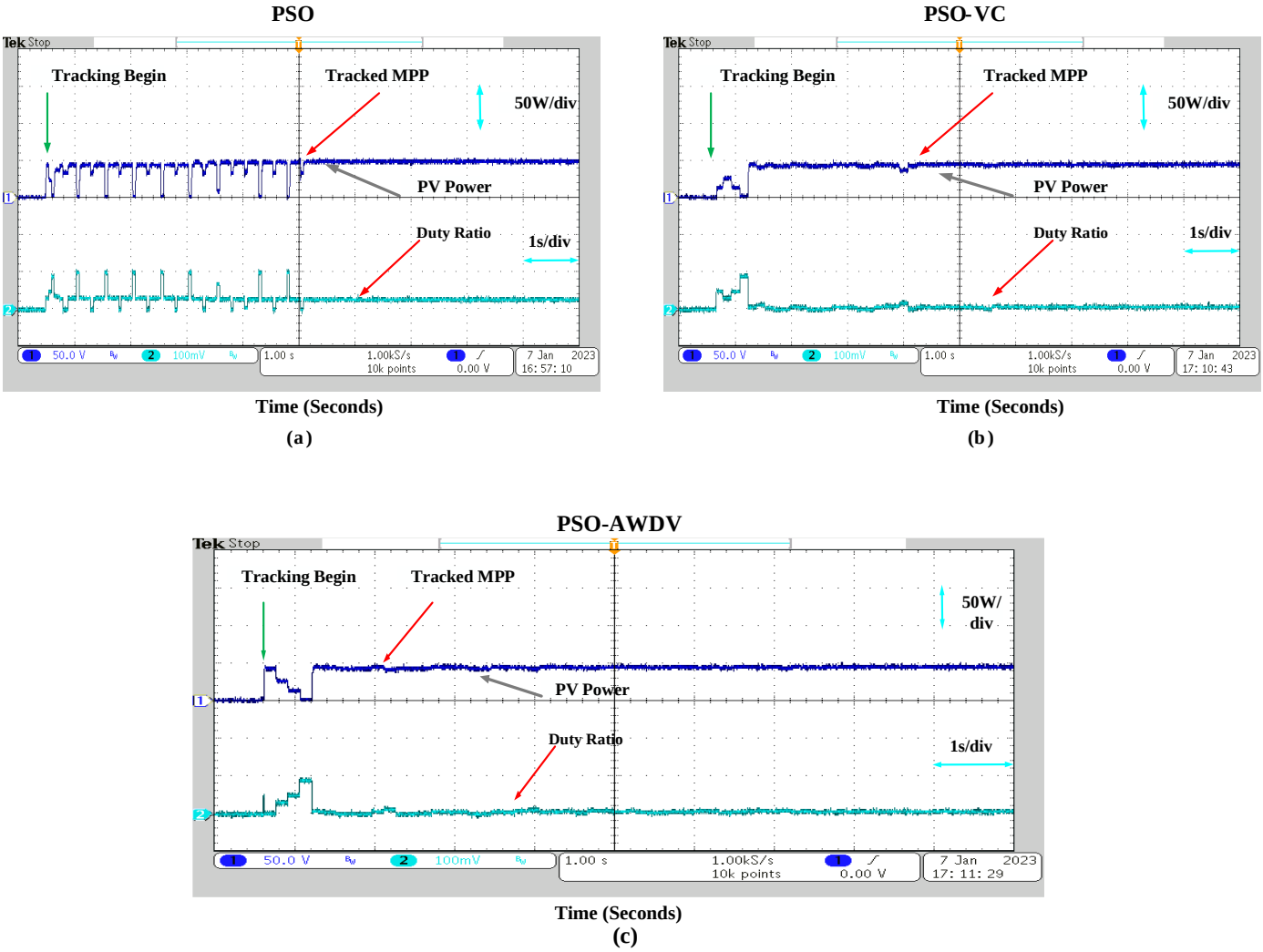


Figure 22. HIL results of (**a**) PSO, (**b**) PSO-VC, and (**c**) PSO-AWDV-based MPPT at Condition 4.

Figure 23 provides a comprehensive comparison of all algorithms, depicting their tracking time, MPP tracked, and efficiency. The analysis from Figure 23 suggests that both PSO and PSO-VC algorithms exhibit more power losses due to this efficiency being reduced. Moreover, their MPP tracking time is considerably longer, accompanied by significant fluctuations. The suggested PSO-AWDV algorithm, however, exhibits exceptional intelligent search-space management skills. Even in complex PS situations, it can efficiently monitor the MPP with the least amount of tracking time, without sacrificing its typical performance. Therefore, the suggested technique satisfactorily meets the requirements for accurate and efficient MPP tracking.

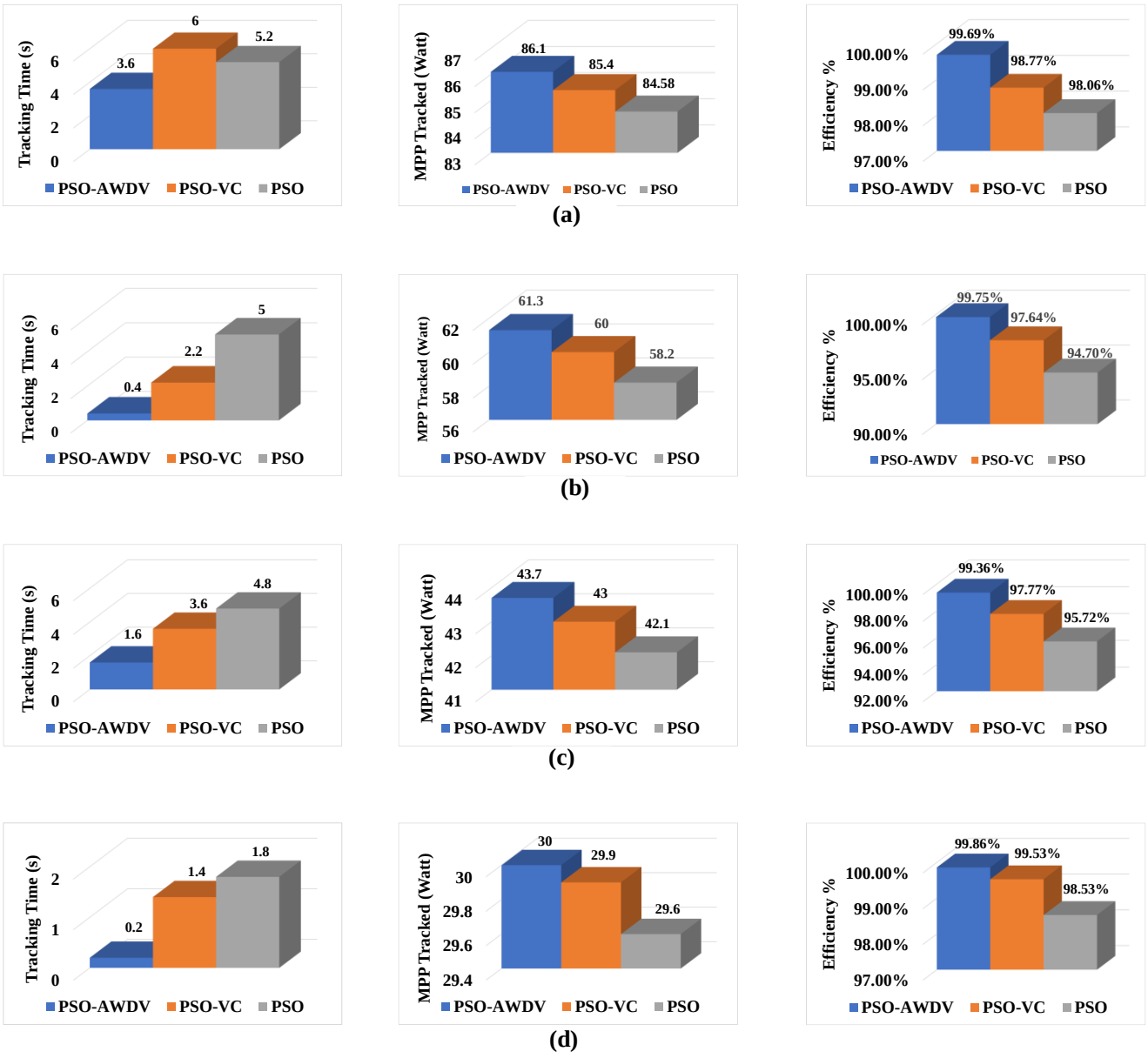


Figure 23. Comparison charts of PSO-AWDV, PSO-VC, and PSO for tracking time, MPP tracked, and efficiency for (**a**) Cond. 1, (**b**) Cond. 2, (**c**) Cond. 3, and (**d**) Cond. 4.

9.2. Dynamic Partial Shading Condition

In this section, we evaluate the PSO-AWDV algorithm's ability to adapt to dynamically changing conditions, making our analysis more practical. We simulate scenarios where shading patterns change due to factors like moving clouds or shifting sun positions over time, using a real-time HIL emulator. Four modules, each rated at 21.837 W, are used in the setup, and each is given a unique shade pattern. Figure 24 presents the performance curves of the PSO-AWDV under various shading conditions, demonstrating how it responds to dynamic changes in insolation, similar to when clouds partially shade the solar panels and then move away, revealing or obscuring the panel's surface. Figure 24 illustrates the transition from Condition 1, characterized by partial shading where panels 1, 2, 3, and 4 receive 1000 W/m^2, 650 W/m^2, 400 W/m^2, and 300 W/m^2, respectively, while in Condition 2 the shading patterns are 1000 W/m^2, 1000 W/m^2, 650 W/m^2, and 350 W/m^2 for four pv module, respectively. The PSO-AWDV converges to the maximum power point (MPP) in around 1.1 s for Condition 1 and 0.6 s for Condition 2. The MPPs tracked in these

conditions are approximately 31.20 W and 50.08 W, with efficiencies of 99.06% and 98.43%, respectively.

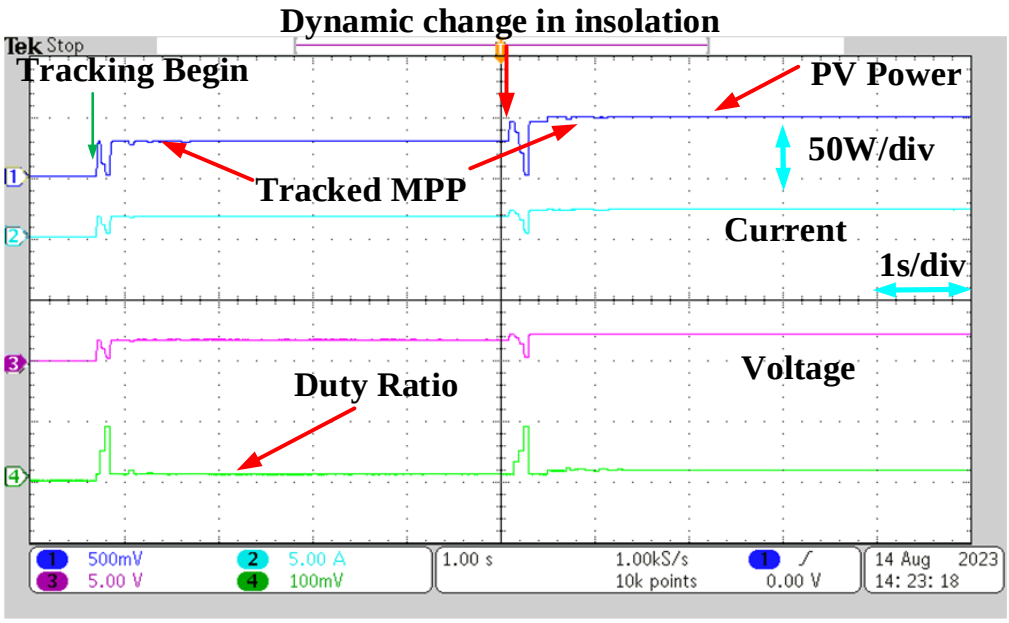


Figure 24. HIL outcome of the PSO-AWDV-based MPPT algorithm when insolation is dynamically changed from 1000, 650, 400, and 300 W/m^2 to 1000, 1000, 650, and 350 W/m^2.

10. Grid Connected Inverter System

The MPPT (maximum power point Tracking) algorithm can be implemented in a grid-connected PV (photovoltaic) system, as depicted in Figure 25. Initially, the solar PV system is linked to a DC–DC converter, and subsequently, the output of the converter is directed to a grid-connected inverter, which feeds power into the grid. The current is measured and compared to a predefined reference value in this process.

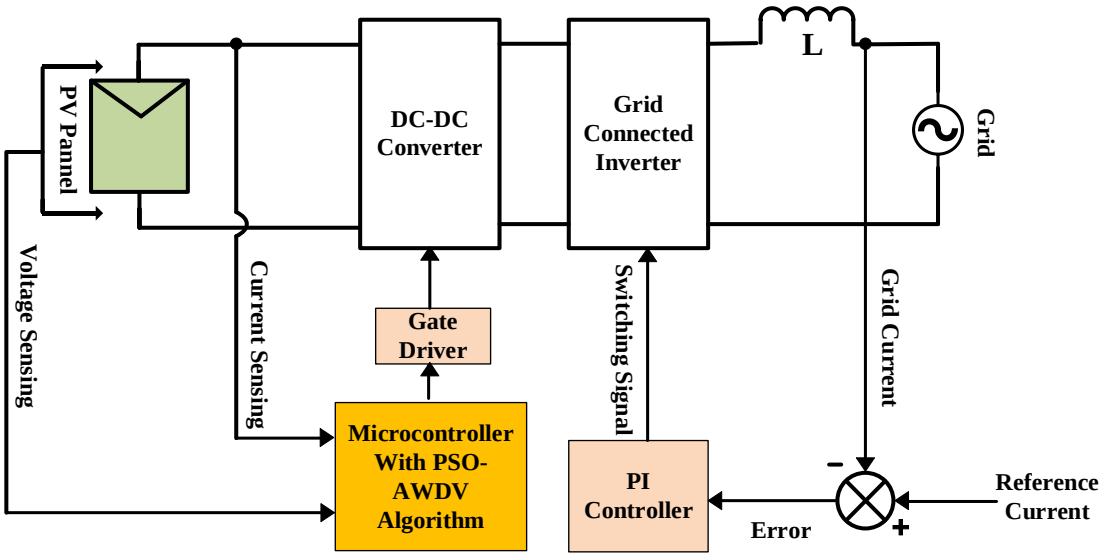


Figure 25. Application of the proposed MPPT Algorithm.

Error is passed through the PI Controller and the switching signal which is generated is given to inverter switches. Current and voltage are sensed and given to the microcontroller unit with the PSO-AWDV algorithm, then it is given to the driver and the switch of the DC–DC converter.

11. Conclusions

This research paper introduces an enhanced approach for improving the performance of MPPT (maximum power point tracking) by combining the conventional particle swarm optimization (PSO) algorithm with the adaptive weighted delay velocity (AWDV) technique. The integration of these two methods aims to address issues such as extended settling times, power fluctuations, and power losses in the MPPT process. As previously mentioned, it surpassed other cutting-edge approaches in terms of a number of parameters, making it the perfect algorithm for MPPT applications. In conclusion, the suggested algorithm showed the following benefits:

- The ability to track time was significantly improved.
- A decrease in power output variations.
- Robustness (performance that remains constant under varying circumstances).
- Reduced oscillations.
- Increased efficiency.

A thorough examination of the proposed algorithm performance was conducted using a four module string in MATLAB/Simulink and real time hardware-in-the-loop (HIL) set up under various shading circumstances. The simulation results clearly indicate that the PSO-AWDV algorithm surpasses other algorithms, including PSO and PSO-VC methods, across various shading conditions. The PSO-AWDV method achieves exceptional performance, boasting a tracking time of 0.42 s and an impressive tracking efficiency of 99.94%. Notably, it manages to track the GMPP without any steady-state oscillations. The Typhoon hardware-in-the-loop (HIL) 402 emulator presented in this study offers a distinct real-time analysis platform of various MPPT methods. The outcomes show that, under all four scenarios, the proposed PSO-AWDV-based MPPT approach achieves extraordinary GMPP tracking having remarkable tracking speed and convergence capability. The oscillations are specifically avoided, reducing power losses and preserving high efficiency.

With an average efficiency of 99.665%, the average PSO-AWDV convergence time to the GMPP is 1.45 s. It should be noted that the effectiveness of PSO-AWDV might be influenced by specific problem formulations, limiting its applicability to different PV systems and configurations. The use of the suggested PSO-AWDV-based MPPT technique in grid-connected systems, as seen in Figure 25 above, might be investigated further.

Author Contributions: Conceptualization, M.T. and A.S.; formal analysis, M.A.A., M.T., A.S., S.A., F.I.B. and A.E.S.; investigation, M.A.A., M.T. and A.S.; methodology, M.A.A., M.T., A.S. and S.A.; supervision, M.T. and A.S.; validation, M.A.A., M.T. and A.S.; writing—original draft, M.A.A.; writing—review and editing, M.T., A.S., S.A., F.I.B., I.S. and A.E.S. All authors have read and agreed to the published version of the manuscript.

Funding: This research has received funding from King Saud University through Researchers Supporting Project number RSP2023R387), King Saud University, Riyadh, Saudi Arabia.

Institutional Review Board Statement: Not applicable.

Informed Consent Statement: Not applicable.

Data Availability Statement: Not applicable.

Acknowledgments: The authors extend their appreciation to King Saud University for funding this work through Researchers Supporting Project number (RSP2023R387), King Saud University, Riyadh, Saudi Arabia.

Conflicts of Interest: The authors declare no conflict of interest.

References

1. Husain, M.A.; Tariq, A.; Hameed, S.; Bin Arif, M.S.; Jain, A. Comparative assessment of maximum power point tracking procedures for photovoltaic systems. *Green Energy Environ.* **2017**, *2*, 5–17. [CrossRef]
2. Abdollahzadeh, B.; Gharehchopogh, F.S.; Khodadadi, N.; Mirjalili, S. Mountain Gazelle Optimizer: A New Nature-inspired Metaheuristic Algorithm for Global Optimization Problems. *Adv. Eng. Softw.* **2022**, *174*, 103282. [CrossRef]

3. Sadeeq, H.T.; Abdulazeez, A.M. Giant Trevally Optimizer (GTO): A Novel Metaheuristic Algorithm for Global Optimization and Challenging Engineering Problems. *IEEE Access* **2022**, *10*, 121615–121640. [CrossRef]
4. Alanazi, A.; Alanazi, M.; Arabi, S.; Sarker, S. A New Maximum Power Point Tracking Framework for Photovoltaic Energy Systems Based on Remora Optimization Algorithm in Partial Shading Conditions. *Appl. Sci.* **2022**, *12*, 3828. [CrossRef]
5. Zhu, W.; Shang, L.; Li, P.; Guo, H. Modified hill climbing MPPT algorithm with reduced steady-state oscillation and improved tracking efficiency. *J. Eng.* **2018**, *2018*, 1878–1883. [CrossRef]
6. Nejila, V.P.; Selvakumar, A.I. Fuzzy-logic based hill-climbing method for maximum power point tracking in PV systems. In Proceedings of the 2013 International Conference Power, Energy Control, ICPEC 2013, Dindigul, India, 6–8 February 2013; pp. 8–13.
7. Hohm, D.P.; Ropp, M.E. Comparative study of maximum power point tracking algorithms. *Prog. Photovolt. Res. Appl.* **2003**, *11*, 47–62. [CrossRef]
8. Osman, M.H.; Ahmed, M.K.; Refaat, A.; Korovkin, N.V. A Comparative Study of MPPT for PV System Based on Modified Perturbation & Observation Method. In Proceedings of the 2021 IEEE Conference of Russian Young Researchers in Electrical and Electronic Engineering (ElConRus), St. Petersburg/Moscow, Russia, 26–29 January 2021.
9. Eltamaly, A.M.; Al-Saud, M.S.; Abokhalil, A.G.; Farh, H.M.H. Simulation and experimental validation of fast adaptive particle swarm optimization strategy for photovoltaic global peak tracker under dynamic partial shading. *Renew. Sustain. Energy Rev.* **2020**, *124*, 109719. [CrossRef]
10. Balamurugan, M.; Narendiran, S.; Sahoo, S.K.; Das, R.; Sahoo, A.K. Application of particle swarm optimization for maximum power point tracking in PV system. In Proceedings of the 2016 3rd International Conference on Electrical Energy Systems (ICEES), Chennai, India, 17–19 March 2016; pp. 35–38.
11. Gupta, A.; Kumar, P.; Pachauri, R.K.; Chauhan, Y.K. Performance Analysis of Neural Network and Fuzzy Logic Based MPPT Techniques for Solar PV Systems. In Proceedings of the 2014 6th IEEE Power India International Conference (PIICON), Delhi, India, 5–7 December 2014; pp. 1–6.
12. Kumar, V.; Kumar, P.; Srinivasa, S.; Puranik, C.R. Study the Effect of Partial Shading in Solar Photovoltaic System. *Int. J. Eng. Res. Technol. IJERT* **2019**, *7*, 1–5.
13. Pervez, I.; Pervez, A.; Tariq, M.; Sarwar, A.; Chakrabortty, R.K.; Ryan, M.J. Rapid and Robust Adaptive Jaya (Ajaya) Based Maximum Power Point Tracking of a PV-Based Generation System. *IEEE Access* **2021**, *9*, 48679–48703. [CrossRef]
14. Megantoro, P.; Nugroho, Y.D.; Anggara, F.; Rusadi, E.Y. Simulation and Characterization of Genetic Algorithm Implemented on MPPT for PV System under Partial Shading Condition. In Proceedings of the 2018 3rd International Conference on Information Technology, Information System and Electrical Engineering (ICITISEE), Yogyakarta, Indonesia, 13–14 November 2018; pp. 74–78.
15. Sarvi, M.; Azadian, A. A comprehensive review and classified comparison of MPPT algorithms in PV systems. *Energy Syst.* **2021**, *13*, 281–320. [CrossRef]
16. Sheraz, M.; Abido, M.A. An Efficient MPPT controller Using Differential Evolution and Neural Network. In Proceedings of the 2012 IEEE International Conference on Power and Energy (PECon), Kota Kinabalu, Malaysia, 2–5 December 2012; pp. 2–5.
17. Sagonda, A.F.; Folly, K.A. A comparative study between deterministic and two meta-heuristic algorithms for solar PV MPPT control under partial shading conditions. In *Power Electronics Handbook*; Elsevier: Amsterdam, The Netherlands, 2022. [CrossRef]
18. Devarakonda, A.K.; Karuppiah, N.; Selvaraj, T.; Balachandran, P.K.; Shanmugasundaram, R.; Senjyu, T. A Comparative Analysis of Maximum Power Point Techniques for Solar Photovoltaic Systems. *Energies* **2022**, *15*, 8776. [CrossRef]
19. Harrison, A.; Alombah, N.H.; de Dieu Nguimfack Ndongmo, J. A New Hybrid MPPT Based on Incremental Conductance-Integral Backstepping Controller Applied to a PV System under Fast-Changing Operating Conditions. *Hindawi Int. J. Photoenergy* **2023**, *2023*, 9931481. [CrossRef]
20. Priyadarshi, N.; Padmanaban, S.; Holm-Nielsen, J.B.; Blaabjerg, F.; Bhaskar, M.S. An Experimental Estimation of Hybrid ANFIS–PSO- Based MPPT for PV Grid Integration Under Fluctuating Sun Irradiance. *IEEE Syst. J.* **2020**, *14*, 1218–1229. [CrossRef]
21. Priyadarshi, N.; Padmanaban, S.; Bhaskar, M.S.; Blaabjerg, F.; Holm-Nielsen, J.B.; Azam, F.; Sharma, A.K. A Hybrid Photovoltaic-Fuel Cell-Based Single Stage Grid Integration with Lyapunov Control Scheme. *IEEE Syst. J.* **2019**, *14*, 3334–3342. [CrossRef]
22. Sajid, I.; Gautam, A.; Sarwar, A.; Tariq, M.; Liu, H.-D.; Ahmad, S.; Lin, C.-H.; Sayed, A.E. Optimizing Photovoltaic Power Production in Partial Shading Conditions Using Dandelion Optimizer (DO)-Based MPPT Method. *Processes* **2023**, *11*, 2493. [CrossRef]
23. Moayedi, H.; Rezaei, A. The feasibility of PSO–ANFIS in estimating bearing capacity of strip foundations rested on cohesionless slope. *Neural. Comput. Appl.* **2021**, *33*, 4165–4177. [CrossRef]
24. Jasim, S.S.; Abdul Hassan, A.K.; Turner, S. Driver Drowsiness Detection Using Gray Wolf Optimizer Based on Face and Eye Tracking. *Aro-Sci. J. Koya Univ.* **2022**, *10*, 49–56. [CrossRef]
25. Ali, K.; Khan, Q.; Ullah, S.; Khan, I.; Khan, L. Nonlinear robust integral backstepping based MPPT control for stand-alone photovoltaic system. *PLoS ONE* **2020**, *15*, e0231749. [CrossRef] [PubMed]
26. Khan, R.; Khan, L.; Ullah, S.; Sami, I.; Ro, J.-S. Backstepping Based Super-Twisting Sliding Mode MPPT Control with Differential Flatness Oriented Observer Design for Photovoltaic System. *Electronics* **2020**, *9*, 1543. [CrossRef]
27. Ali, K.; Khan, L.; Khan, Q.; Ullah, S.; Ali, N. Neurofuzzy robust backstepping based MPPT control for photovoltaic system. *Turk. J. Electr. Eng. Comput. Sci.* **2021**, *29*, Article 27. [CrossRef]

28. Raiker, G.A.; Loganathan, U.; Reddy, S.B. Current Control of Boost Converter for PV Interface With Momentum-Based Perturb and Observe MPPT. *IEEE Trans. Ind. Appl.* **2021**, *57*, 4071–4079. [CrossRef]
29. Baimel, D.; Tapuchi, S.; Levron, Y.; Belikov, J. Improved Fractional Open Circuit Voltage MPPT Methods for PV Systems. *Electronics* **2019**, *8*, 321. [CrossRef]
30. Bharath, K.R.; Suresh, E. Design and Implementation of Improved Fractional Open Circuit Voltage Based Maximum Power Point Tracking Algorithm for Photovoltaic Applications. *Intern. J. Renew. Energy Res. IJRER* **2017**, *7*, 1108–1113.
31. Zaghba, L.; Khennane, M.; Borni, A.; Fezzani, A. Intelligent PSO-Fuzzy MPPT approach for Stand Alone PV System under Real Outdoor Weather Conditions. *Alger. J. Renew. Energy Sustain. Dev.* **2021**, *3*, 1–12. [CrossRef]
32. Rajalashmi, C.K.; Monisha, C. Maximum Power Point Tracking Using Ant Colony Optimization for Photovoltaic System Under Partially Shaded Conditions. *Int. J. Eng. Adv. Technol. IJEAT* **2018**, *8*, 82–87.
33. Mirza, A.F.; Mansoor, M.; Ling, Q.; Yin, B.; Javed, M.Y. A Salp-Swarm Optimization based MPPT technique for harvesting maximum energy from PV systems under partial shading conditions. *Energy Convers. Manag.* **2020**, *209*, 112625. [CrossRef]
34. Singh, N.; Gupta, K.K.; Jain, S.K.; Dewangan, N.K.; Bhatnagar, P. A Flying Squirrel Search Optimization for MPPT Under Partial Shaded Photovoltaic System. *IEEE J. Emerg. Sel. Top. Power Electron.* **2020**, *9*, 4963–4978. [CrossRef]
35. Altamimi, S.N.; Feilat, E.A.; al Nadi, D.A. Maximum Power Point Tracking Technique Using Combined Incremental Conductance and Owl Search Algorithm. In Proceedings of the 2021 12th International Renewable Engineering Conference (IREC), Amman, Jordan, 14–15 April 2021; pp. 1–6.
36. Farzaneh, J.; Keypour, R.; Khanesar, M.A. A New Maximum Power Point Tracking Based on Modified Firefly Algorithm for PV System Under Partial Shading Conditions. *Technol. Econ. Smart Grids Sustain. Energy* **2018**, *3*, 9. [CrossRef]
37. Sutikno, T.; Subrata, A.C.; Elkhateb, A. Evaluation of Fuzzy Membership Function Effects for Maximum Power Point Tracking Technique of Photovoltaic System. *IEEE Access* **2021**, *9*, 109157–109165. [CrossRef]
38. Azad, M.L.; Das, S.; Sadhu, P.K.; Arvind, P. High-Performance Algorithms to Ascertain The Power Generation In A Photovoltaic System Using Fuzzy Logic Controller. In Proceedings of the 2020 International Conference on Intelligent Engineering and Management (ICIEM), London, UK, 17–19 June 2020; pp. 425–430.
39. Raj, A.; Gupta, M. Numerical Simulation and Performance Assessment of ANN-INC Improved Maximum Power Point Tracking System for Solar Photovoltaic System Under Changing Irradiation Operation. *Ann. RSCB* **2021**, *25*, 790–797.
40. Chao, K.-H.; Rizal, M. A Hybrid MPPT Controller Based on the Genetic Algorithm and Ant Colony Optimization for Photovoltaic Systems under Partially Shaded Conditions. *Energies* **2021**, *14*, 2902. [CrossRef]
41. Babu, K.G.; Kishori, K.R. MPPT design using grey wolf optimization differential evolution (GWODE) technique for partially shaded PV system. *Int. J. Emerg. Technol. Innov. Res.* **2018**, *5*, 203–218.
42. Bhuvaneswari, G.; Annamalai, R. Development of a solar cell model in MATLAB for PV based generation system. In Proceedings of the 2011 Annual IEEE India Conference Sustainable Engineering Solutions INDICON-2011, Hyderabad, India, 16–18 December 2011.
43. Asim, M.; Tariq, A.; Tariq, M. Simulink based modeling, simulation and performance evaluation of an MPPT for maximum power generation on resistive load. In Proceedings of the 2011 2nd International Conference on Environmental Science and Technology, Singapore, 26–28 February 2011; IPCBEE: Singapore, 2011.
44. Magdaleno, R.S.; Sánchez-Pérez, P.A.; Cruz, J.R.; Escobar, D.M.; Sánchez-Juárez, A. Influence of partial shading on the power output of a solar cell and a PV module. In Proceedings of the 2018 IEEE 7th World Conference on Photovoltaic Energy Conversion (WCPEC) (A Joint Conference of 45th IEEE PVSC, 28th PVSEC & 34th EU PVSEC), Waikoloa Village, HI, USA, 10–15 June 2018; pp. 1324–1327.
45. Ramaprabha, R.; Mathur, B.L. Characteristics of solar PV array under partial shaded conditions. In Proceedings of the TENCON 2008 IEEE Region 10 Conference, Hyderabad, India, 19–21 November 2008.
46. Liu, Y.-H.; Huang, S.-C.; Huang, J.-W.; Liang, W.-C. A Particle Swarm Optimization-Based Maximum Power Point Tracking Algorithm for PV Systems Operating Under Partially Shaded Conditions. *IEEE Trans. Energy Convers.* **2012**, *27*, 1027–1035. [CrossRef]
47. Koad, R.B.A.; Zobaa, A.; El-Shahat, A. A Novel MPPT Algorithm Based on Particle Swarm Optimization for Photovoltaic Systems. *IEEE Trans. Sustain. Energy* **2016**, *8*, 468–476. [CrossRef]
48. Xu, L.; Song, B.; Cao, M. An improved particle swarm optimization algorithm with adaptive weighted delay velocity. *Syst. Sci. Control Eng.* **2021**, *9*, 188–197. [CrossRef]
49. Ratnaweera, A.; Halgamure, S.K.; Watson, H.C. Self-organizing herarchical particle swarm optimizer with time-varying acceleration coefficients. *IEEE Trans. Evol. Comput.* **2004**, *8*, 240–255. [CrossRef]

Disclaimer/Publisher's Note: The statements, opinions and data contained in all publications are solely those of the individual author(s) and contributor(s) and not of MDPI and/or the editor(s). MDPI and/or the editor(s) disclaim responsibility for any injury to people or property resulting from any ideas, methods, instructions or products referred to in the content.